Chapter 6

Congenital Abnormalities of the Fetal Heart

Dominic Gabriel Iliescu, Ștefania Tudorache,
Dragos Nemescu, Monica Mihaela Cirstoiu,
Simona Vlădăreanu, Claudiu Marginean,
Iuliana Ceausu, Daniel Muresan,
Marius Calomfirescu Vicea, Mona Elena Zvanca,
Cezara Muresan, Laura Monica Cara,
Ciprian Laurentiu Patru,
Roxana Cristina Drăgușin and Maria Sorop-Florea

Additional information is available at the end of the chapter

http://dx.doi.org/10.5772/intechopen.74077

Abstract

Congenital heart defects (CHDs) are the most frequent congenital malformations, the costliest hospital admissions for structural defects and the leading cause of infant general and malformations related mortality. Fetal echocardiography represents a skilled ultrasound examination, because of the complexity, physiological and structural particularities of the fetal heart. The efficiency of the cardiac scan is reported with great variation, depending on the scanning protocol, examiner experience and equipment quality but CHDs remains among the most frequently missed congenital abnormalities.

Keywords: heart defects, congenital, ultrasonography, echocardiography

1. Epidemiology. Incidence and risk factors for cardiac abnormalities

Congenital heart defects (CHD) are the most frequent congenital malformations (5–12 per 1000 live births), the costliest hospital admissions for structural defects and represent the leading cause of infant general and malformations related mortality (42%) [1, 2]. Prenatal CHD detection allows proper counseling, provides the options of pregnancy termination [3], in utero treatments (antiarrhythmics, valvuloplasties, etc.) [4–7] and allows for delivery planning in a referral center [8–11].

CHD etiology includes many genetic, environmental and teratogenic factors [12–16], but 90% of heart malformations have no identified cause. Conversely, the risk may be reduced with periconceptionally folic acid intake [17].

2. Indications and settings for fetal echocardiography (FECG)

A detailed sonographic examination, used to characterize fetal cardiac anatomy has traditionally been reserved for high-risk populations [18–22]: advanced maternal age, more than 35 years old, family history of CHD or disorders that involves potential CHD, infectious, autoimmune or metabolic diseases, exposure to drugs and teratogens. FECG was also proposed in certain pregnancy findings: structural defects, non-immune hydrops, arrhythmia, suspected chromosomal abnormalities, enlarged nuchal translucency, monochorionic multiple gestation. Nowadays, professional guidelines recommend a screening heart evaluation to all pregnancies, as most of the CHD cases are not associated with known risk factors [38–45].

Guidelines and training requirements have been developed [18, 19]. An accurate visualization of heat features is commonly achieved at 18–22 gestational weeks. FECG is a relatively brief but skilled ultrasound examination, because of the complexity and prenatal physiological and structural particularities of the fetal heart. Consequently, FECG has not been widely implemented, and the prenatal diagnosis of even severe CHD varies considerably, with less than half prenatally detected.

3. Fetal heart evaluation. The cardiac sweep and longitudinal views

Optimal views of the fetal heart are obtained when the cardiac apex is orientated toward the anterior maternal wall. Heart anatomy is evaluated using a sequential segmental analysis, starting from the venous plane (atria with veins connections), following the blood flow to ventricles and great arteries [23]. The information regarding fetal heart anatomy is achieved by examining five axial and three longitudinal scanning planes [18, 19, 24], described below, with examples of cardiac abnormalities. In general practice, only the axial sectional planes are evaluated during the cardiac sweep [25] (**Figure 1**).

1. **Upper abdominal view** facilitates the evaluation of normal abdominal situs by identifying the stomach, descending aorta and inferior vena cava position (**Figure 1(1)**).
2. **Four-chamber view (4CV)** is visualized in the lower half of the fetal chest, where the heart, with crux cordis occupying its central portion and a complete rib are present (**Figure 1(2)**). The evaluation parameters include:
    - *Situs*—the heart is normally left-sided, namely levocardia, or situs solitus. Rarely, a complete situs inversus is present. In the presence of an abnormal heart situs CHD but also congenital diaphragmatic hernia should be considered (**Figure 2**), as the presence of significant ectopic abdominal content in the chest displaces the heart.

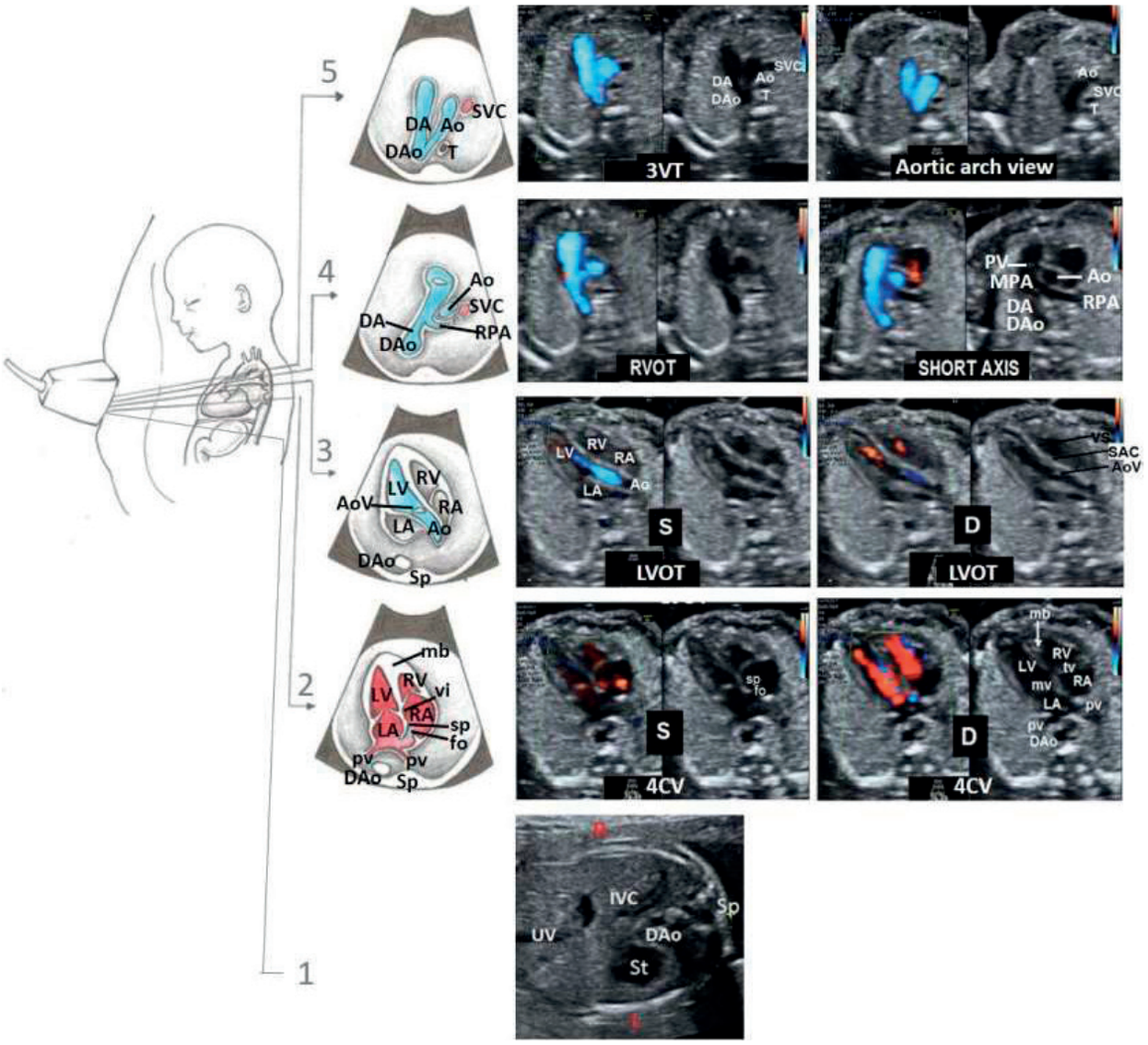

Figure 1. Normal heart visualized during fetal cardiac sweep. Visualization of the cardiac transverse planes, by sweeping the transducer from the four-chamber plane toward the fetal neck as shown in the left of the image. Schematic presentation of the cardiac planes in duplex mode (gray-scale and color Doppler) that become apparent: (1) upper abdominal view, and abdominal situs; (2) four-chamber view (4CV). The atrioventricular Doppler flow is red because of the direction toward the direction during diastole. When the atrioventricular are closed, during systole, the atrioventricular flow is absent; (3) left ventricular outflow tract (LVOT). Note the continuity of the ventricular septum (VS) with the aortic wall. When the aortic valve (AoV) is closed, during diastole, the aortic flow is absent; (4) right ventricular outflow tract (RVOT) and (5) three-vessel and trachea (3VTV) and aortic arch views. L, left; R, right; St, stomach; D, diastole; and S, systole; UV, umbilical vein; DAo, descending aorta; IVC, inferior vena cava; SVC, superior vena cava; LV, left ventricle; RV, right ventricle; LA, left atrium; RA, right atrium; mb, moderator band; mv, mitral valve; tv, tricuspid valve; vi, valve insertion; pv, pulmonary veins; sp., septum primum; fo, foramen ovale, DAo, descendent aorta; MPA, main pulmonary artery; DA, ductus arteriosus; RPA, right pulmonary artery; PV, pulmonary valve Sp, spine; T, trachea. Modified with permission [26].

- *Heart axis*—normally, the apex points toward the left side at 45 ± 15–20° (**Figure 1(2)**). Some studies on CHDs suggested that an abnormal cardiac axis is present in more than two-thirds of the cases [27] (**Figure 15C**).
- *Area of the heart*, is abnormally increased if higher than 1/3 of the thorax area, or cardio-thoracic circumference ratio is above two standard deviations [28] (**Figure 3**). It can arise

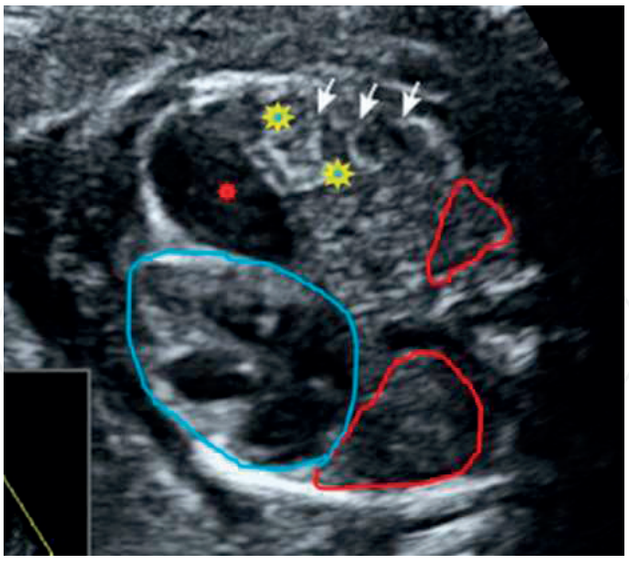

Figure 2. Two-dimensional US images in the cross-sectional plane of the thorax at the level of the four-chamber view of the heart. Stomach (red star) and small bowel loops (yellow stars) are identified intrathoracic and displaces fetal heart (figured by the blue tracing line) to the right; the lungs areas are highlighted by red tracing lines. With permission, Tudorache et al. [34].

from a number of situations which include CHD, particularly tricuspid atresia or dysplasia, including Ebstein's anomaly, twin to twin transfusion syndrome, fetal dilated cardiomyopathies, hydrops fetalis, or may be due to abnormal shunting from arteriovenous malformations, as the vein of Galen malformation or placental chorioangioma (**Figure 3**).

- *The atria* present similar size. The pulmonary veins enter the posterior left atrium and both vena cava enter the anterior right atrium (**Figure 1(2)**). Various condition may alter this spatial relation, as fetal isomerism and the normal atrial dimensions, where Ebstein's anomaly is the most representative condition (**Figure 4**).

- *The ventricles* should be visualized with similar width and contractility. The right ventricle is anterior, with more coarse lining and trabeculation. Abnormal shape of the ventricular wall lining may be an indicator for cardiac tumors, as tuberous sclerosis (**Figure 5**) or rhabdomyoma (**Figure 6**). Normally, the left ventricle forms the apex of the heart, the right ventricular apex contains the moderator band and septal insertion of the tricuspid valve is more apical than the mitral valve (**Figure 1(2)**). In later gestation, the right ventricle becomes slightly larger, but 2D or M-mode nomograms correlated with the gestational age or fetal biometry and Z-scores for fetal heart area and axis and cardiothoracic ratio, atrioventricular valve annuli, ventricular lengths and walls thickness, but also for emerging vessels, are available [29, 30].

  A diminutive ventricle may be associated with significant CHD, as the hypoplastic left/right heart syndrome (**Figure 7**). Also, an abnormally small left ventricle may be an indirect sign of aortic coarctation (**Figure 19A**). However, less significant cardiac abnormalities may associate a larger right heart, as the persistence of left superior vena cava (**Figure 8**).

- *Ventricular septum integrity* is better evaluated from a lateral incidence, with the ultrasound beam perpendicular to the septum. A dropout of echoes or an opening of the

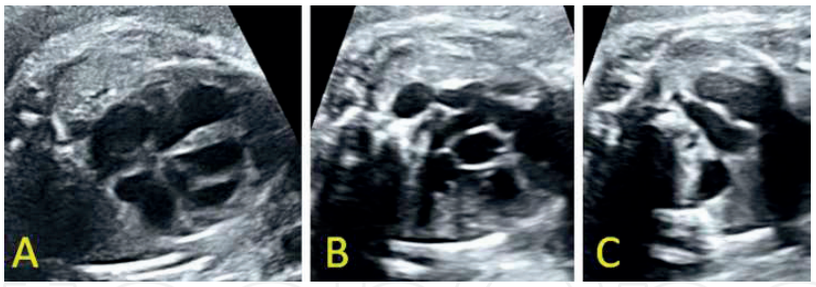

Figure 3. Cardiomegaly. (A) Increased area of the heart, occupying half of the thorax area. (B and C):Outflow tract appears dilated in relation to the fetal thorax.

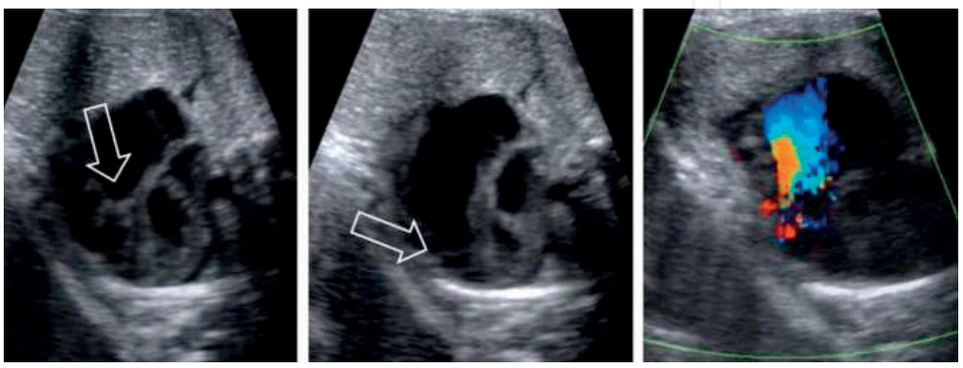

Figure 4. Ebstein's anomaly. The arrow indicates the dysplastic tricuspid valve with septal and posterior leaflets of the tricuspid valve displaced toward the apex of the right ventricle. Color Doppler investigation shows significant valvular regurgitation.

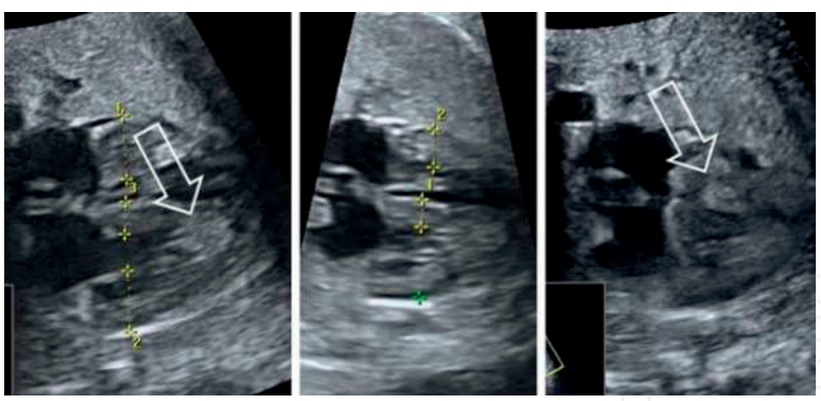

Figure 5. Tuberous sclerosis. Increased thickness of ventricular walls and presence of solid tumors in ventricular cavities, highlighted with open arrows.

ventricular septum, causing communication between the two ventricles suggests the diagnosis. The entire septum must be swept (**Figure 9**) for a more confident diagnosis, and Doppler investigation enhances the diagnosis, especially for small defects (**Figure 10**). Ventricular septal defects are the most common cardiac abnormality and accounts for almost one third of all cardiac defects.

- *Atrial septum primum* presence, at the crux of the heart, along the *atrioventricular valves* insertion which is more apical for tricuspid valve. Atrioventricular septal defects, known

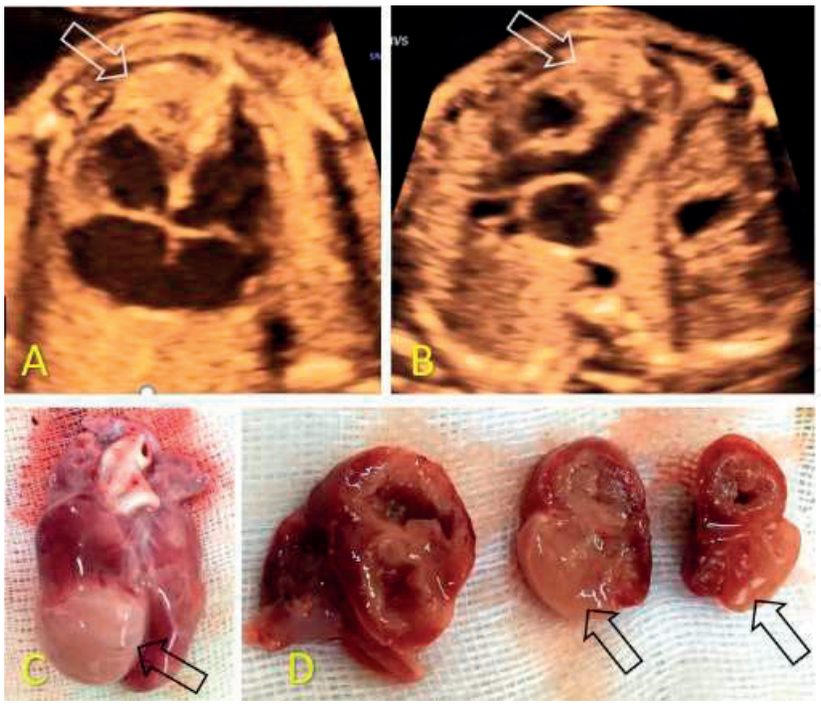

Figure 6. Rhabdomyoma of the right ventricle, visible in 4CV (A) and left ventricle outflow tract view (B), and confirmed postabortum (C and D), penetrating the ventricular wall (C).

as endocardial cushion defects are situated in the central core of the heart. It involves the association of septum primum and ventricular septal defect and a variable degree of abnormal atrioventricular valves (**Figure 11**).

- *Foramen ovale* represents about one third of the atrial septum and the flap bulges in the left atrium. A restrictive foramen ovale, because of a narrow foramen ovale orifice, or premature adhesion of the foramen ovale valve to the atrial septum, has repeatedly been discussed as a cause of fetal hemodynamic compromise [31]. Foramen ovale aneurysm is defined as dilatation of the atrial septum with bulging of the septum at least half the distance to the left atrial wall (**Figure 12**), is primarily a defect of septum primum which results in: septum primum bulging, loss of the normal biphasic motion of foramen ovale and arrhythmia. Associated abnormalities include: atrial septal defect, tricuspid atresia, hypoplastic right heart, aortic stenosis, transposition of the great vessels, Ebstein anomaly, atrioventricular valve and pulmonary venous obstruction.

- *Pericardial effusion* should be absent, or less than 2–4 mm. Greater effusions usually occur as a component of hydrops, as one of the earliest findings, and are also associated with cardiac structural abnormality, arrhythmia and an increased incidence of chromosomal anomalies (**Figure 12**) [32, 33].

- *Heart rate and the regularity* of the rhythm is assessed based on the cardiac cycle length measured using M-mode or pulsed Doppler interrogation. Most common arrhythmias are transient and without clinical relevance, as brief episodes, less than 1–2 minutes of a bradycardic, tachycardic or irregular heart rhythm.

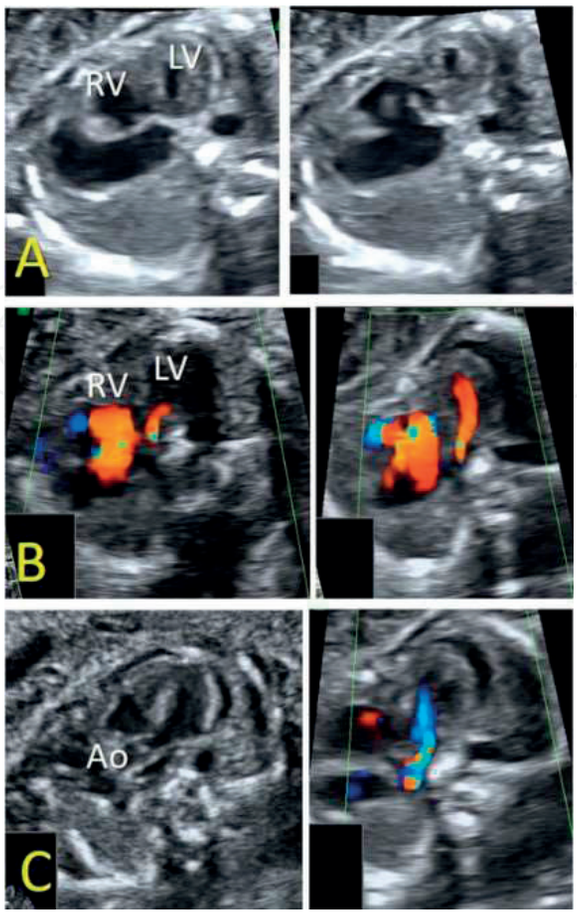

Figure 7. Hypoplastic left heart syndrome (HLHS), with discordance of the heart chambers, ventricular cardiomyopathy and hypertrophic left ventricle (A), markedly reduced filling at Doppler evaluation (B), fibroelastosis, and reduced aortic caliber and flow (C).

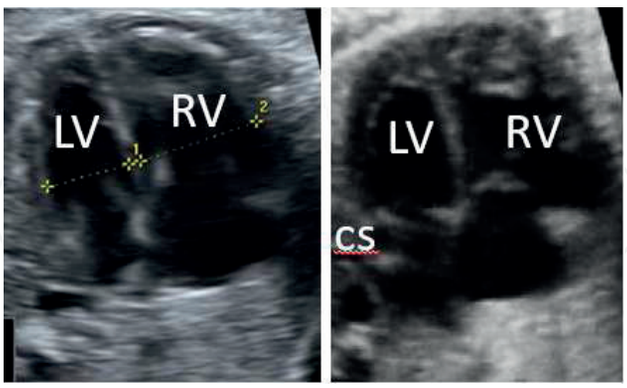

Figure 8. Discordance of the cardiac ventricles, with enlarged right ventricle and dilated coronary sinus (CS), in the presence of persistent left superior vena cava.

Irregular cardiac rhythm represents the most common rhythm anomaly and is almost always associated with isolated premature atrial contractions (PACs). Frequently blocked PACs will result in bradyarrhythmia that can mimic bradycardia (**Figure 13**). In rare cases, irregular rhythm may progress to supraventricular tachycardia.

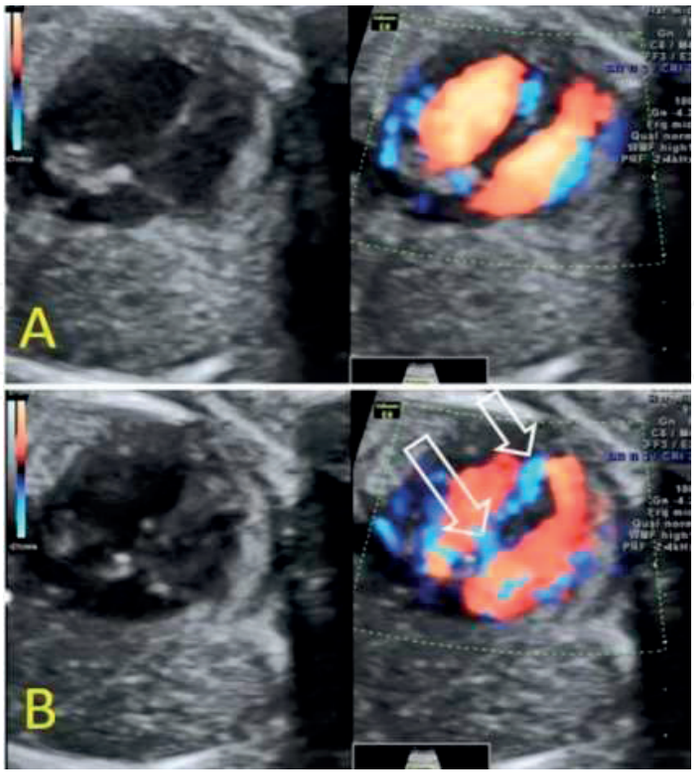

Figure 9. Multiple VSDs, apical and membranous, unapparent in certain 4CV incidence at gray-scale and color Doppler evaluation (A), but present in nearby planes, as the cardiac sweep is conducted (B). The entire interventricular septum must be carefully swept.

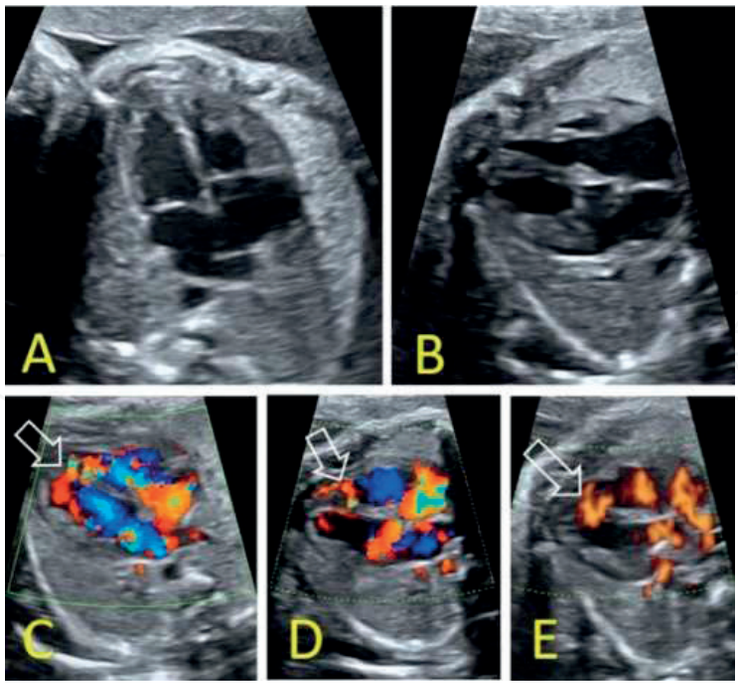

Figure 10. Multiple VSDs, apical and muscular, inapparent in gray-scale evaluation. (A): Apparently normal ventricular septum in apical and (B): lateral four-chamber view. (C–E): Muscular VSDs diagnosed using color Doppler in lateral four-chamber view—open arrows.

http://dx.doi.org/10.5772/intechopen.74077

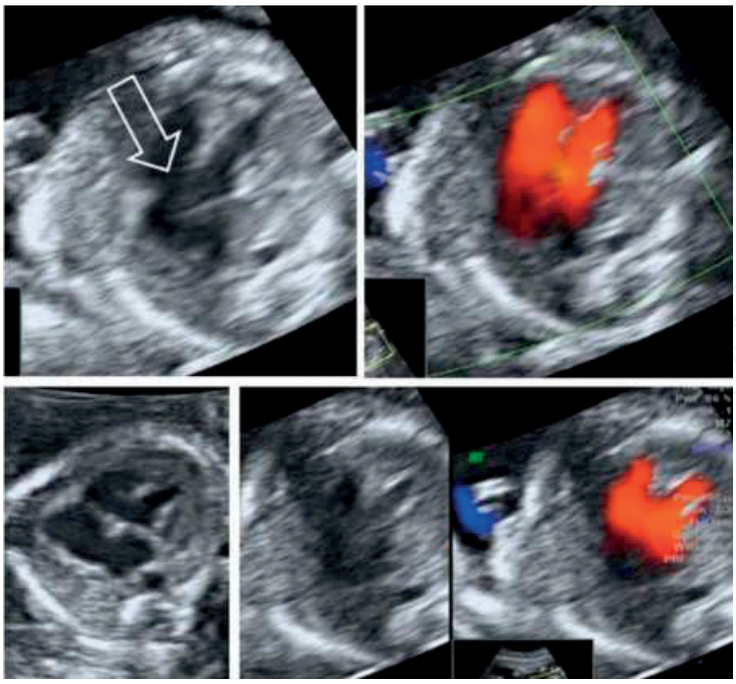

Figure 11. Atrioventricular septal defect. A large defect (open arrow) is present in the area where normally crux cordis is identified.

Fetal bradycardia represents a persistently slower heart rate, of less than 100–120 beats/min. More concerning is the observation of sustained bradycardia induced by sinus bradycardia, atrial bigeminy and complete heart block. Heart block is frequently associated with maternal anti-Ro autoantibodies and CHD and the most common condition is an unbalanced atrioventricular septal defect associated with left isomerism.

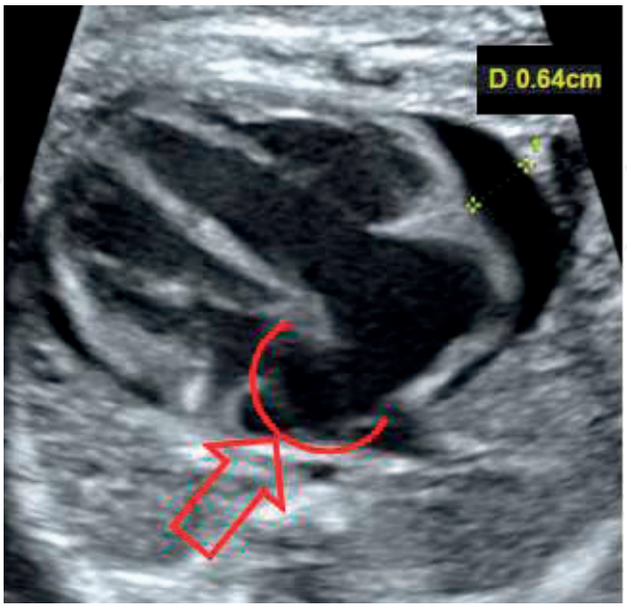

Figure 12. Foramen ovale aneurysm (red arrow) in a case where pericarditis is associated.

Fetal tachycardia implies atrial and ventricular rates above 180 bpm. Fetal anemia, hypoxia, infections, and maternal thyrotoxicosis may induce this condition. The main causes of fetal tachycardia are supraventricular tachycardia (**Figure 14**), the most common cause, with atrioventricular re-entry due to a fast conducting accessory pathway), sinus tachycardia, and atrial flutter (with atrial rate 300–500 bpm and only every second or third atrial beat conducted across the atrioventricular node, resulting in ventricular rates of 150–250 bpm). The use of echocardiography is important to differentiate these conditions and their hemodynamic impact, because the severe conditions may lead to low cardiac output, hydrops and fetal demise.

- *Coronary sinus*, may be demonstrated by fine sweeping caudally from the 4CV (**Figure 8**).

Given all these information, the 4CV is much more than a simple count of cardiac chambers, but certain abnormalities, especially involving great vessels, cannot be detected at the 4CV level alone [35]. Recent revised and updated guidelines and recommendations from several professional bodies [18, 36, 37] plead for the routinely screening evaluation of the outflow tract views along the 4CV, based on strong medical evidence regarding the prenatal detection of CHD [38–40].

3. **Left ventricular outflow tract (LVOT)** is visualized cranially from the 4CV plane and directed toward the fetal right shoulder. In this five-chamber view, the ascending aorta appears arising from the left ventricle (**Figure 1(3)**), with no proximal *transversal branching*, allowing for its differentiation from the main pulmonary artery.

   - *Septoaortic continuity*, should be visualized as a continuous line between ventricular septum and aortic wall. The discontinuity of this structure is seen in the presence of a

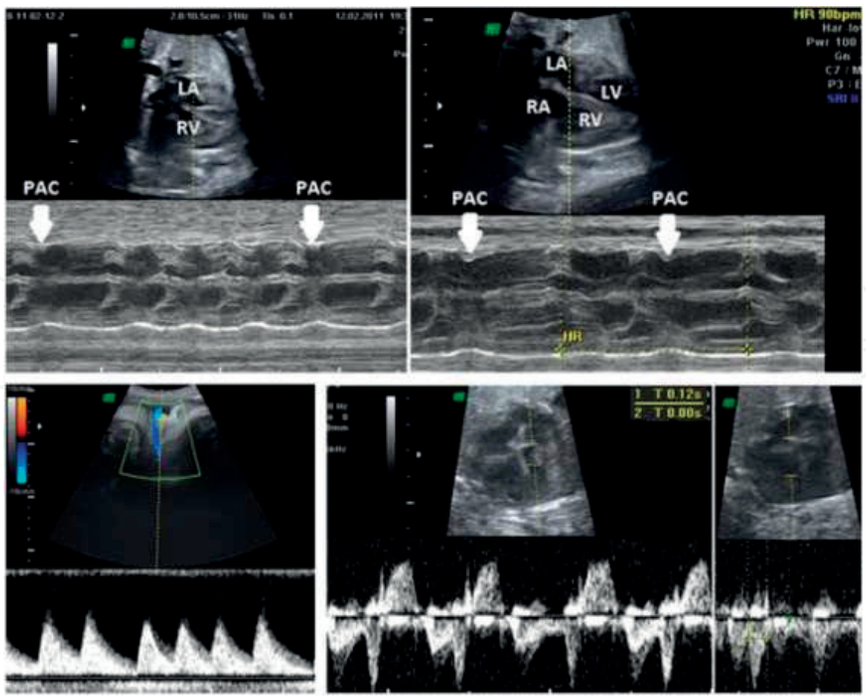

Figure 13. Fetal bradyarrhythmia, M-mode and pulsed Doppler evaluation. Premature atrial contractions (PACs, highlighted with arrows) are blocked, resulting in bradycardic irregular cardiac rhythm. Normal values for the mechanical PR interval by pulsed Doppler interrogation at the mitral-aortic region in prediction of heart block risk.

http://dx.doi.org/10.5772/intechopen.74077

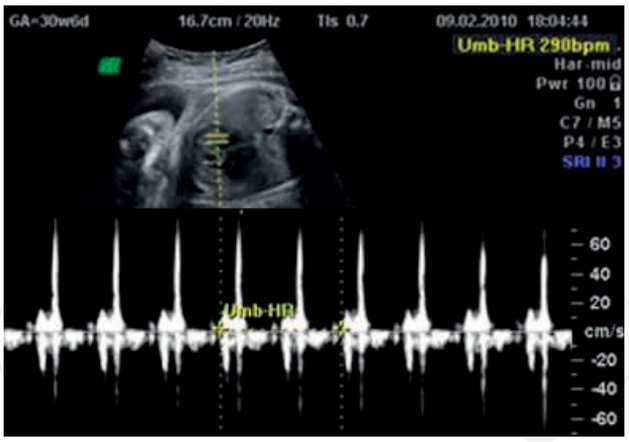

Figure 14. Tachyarrhythmia and measurement of cardiac rhythm using pulsed Doppler.

sub-aortic septal defect that is frequently associated with overriding. A good example of this condition is present in tetralogy of Fallot cases (**Figure 15**).

- The *aortic valve* cusps should open freely, disappearing in systole and not thickened. Aortic dysplastic and stenotic valves do not fully open this will decrease the blood flow into the aorta. Aortic stenosis impairs the left ventricular development, leading to hypoplastic left heart syndrome (**Figure 16**).

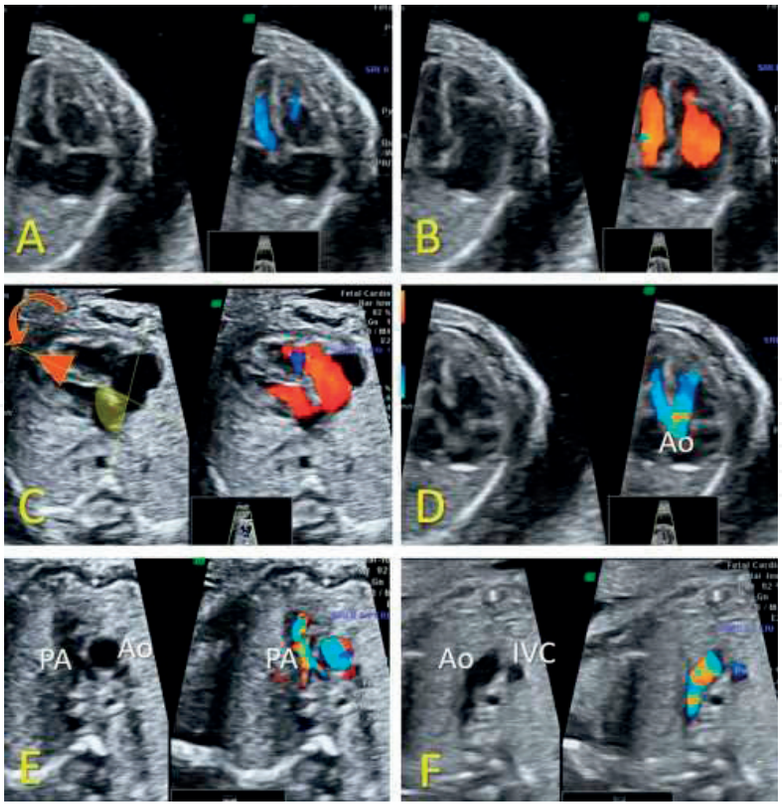

Figure 15. Tetralogy of Fallot. Inapparent four-chamber view (A and B) with increased cardiac axis (C). Septal defect with septoaortic discontinuity and aortic root overriding at the level of mixing flows form ventricles (D). Diminutive stenotic pulmonary artery is identified in right outflow tract view (E) and three-vessel and trachea view (F).

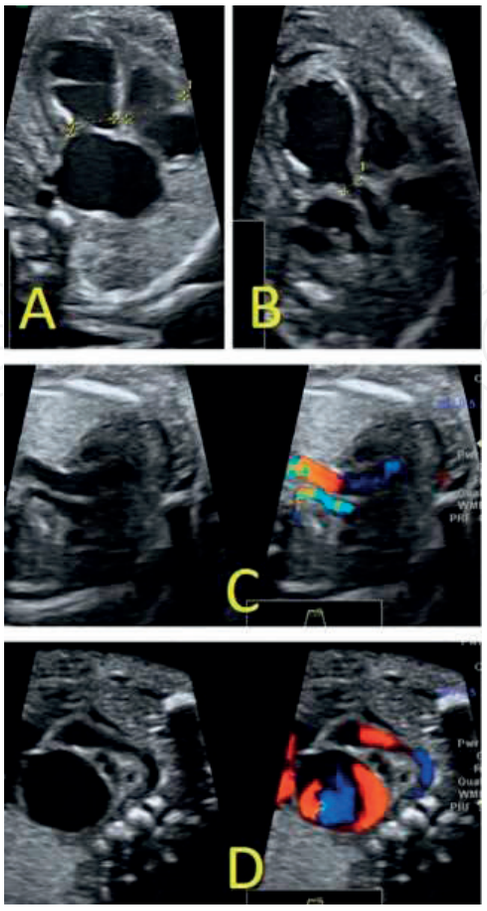

Figure 16. Aortic stenosis. Abnormal left ventricle with atretic inlet and fibroelastosis (A), stenotic aortic root (B) and aortic arch in axial (C) and longitudinal (D) views.

- *The width* of the aorta should be approximately equal with the pulmonary artery. Unbalanced blood flows through the outflow tracts as in Fallot Tetralogy, determine a larger aorta, because the aortic root receives blood from both ventricles due to overriding (**Figure 15D** and **E**). Valvular dysplasia and aortic arch stenosis/coarctation (**Figure 16**) determine a smaller aortic caliber.

4. **Right ventricular outflow tract (RVOT)** and short axis view are visualized cranially from the LVOT plane (**Figure 1(4)**), where the main pulmonary artery root arises from the anterior right ventricle with a short and straight course and soon *branching* into a large vessel, the ductus arteriosus directed straight posteriorly toward the descending aorta as an extension of the main artery, and the smaller pulmonary arteries directed laterally.

   - The pulmonary *valve cusps* should have a similar aspect as described for the aortic valves. The dysplastic stenotic valves may appear thickened and with incomplete opening during systole (doming) (**Figure 17A**) and determine pulmonary stenosis.

   - The approximately equal *width* of the two outflow tracts should be noted. Pulmonary stenosis may be associated with valvular stenosis, total anomalous pulmonary venous drainage, septal defects, supravalvular aortic stenosis, Noonan syndrome and tetralogy of Fallot. On color and pulsed Doppler investigation, pulmonary stenosis cases display turbulent or retrograde flow in and increased velocities distal to the valve (**Figure 17B**

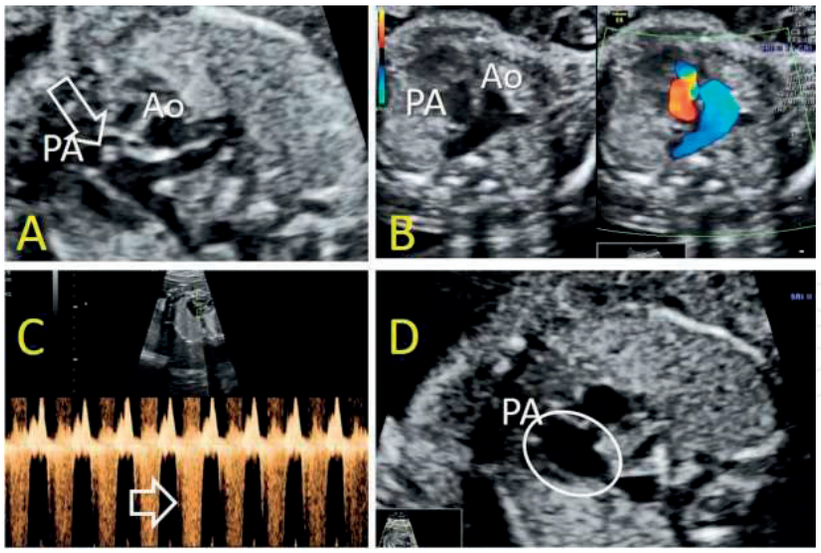

Figure 17. Pulmonary stenosis. (A): Dysplastic pulmonary valves, with incomplete opening and doming; (B): reversed and turbulent flow in the RVOT; (C): post-stenotic increased velocities in pulmonary artery course; (D): post-stenotic dilatation.

and **C**), with PSV higher than the aortic flow. A post-stenotic dilatation of the proximal pulmonary artery may be seen (**Figure 17D**). A variable degree of hypoplastic right ventricle with hypertrophic wall, dilatation of the right atrium, and tricuspid insufficiency may be present, while congestive heart failure and hydrops may occur in severe stenosis.

- *Spatial relationship* evaluation should note crossing of aorta at a right angle and characteristic early transversal branching of the pulmonary artery (**Figure 1(4)**). In the absence of these ultrasound features, transposition of the great arteries should be suspected (**Figure 18**).

5. **Three-vessel and trachea view (3VTV)** is obtained sliding cranially in the upper thorax during cardiac sweep (**Figure 1(5)**). Superior vena cava (SVC) on the right side, the aortic arch and ductal arch, anterior and to the left of the aorta, are visualized. The approximately equal arterial arches form a *"V"-shaped confluence* toward the descending aorta, in the left of the spine. This plane is also used for thymus evaluation [41].

   This view may be altered with regard to several features. Their width may be discrepant, as due to aortic coarctation, where the aortic isthmus is significantly smaller than the arterial duct (**Figure 19**). However, this diagnosis is challenging and affected by high rates of false-positive diagnoses. Thus, to improve detection, a multiple-criteria prediction model is adopted, as a combination of isthmic/duct and ventricular diameters ratios and Z-scores, visualization of CoA shelf and isthmic flow disturbance [42, 43].

   Another abnormality of 3VTV plane is represented by the impossibility to identify all the three vessels. One of the arterial arches may not be seen, as in the presence of an interrupted aortic arch (**Figure 20**), or more than three vessels may be present, as in persistent left superior vena cava (**Figure 21**).

   The superior vena cava may be identified contralateral, on the left side, as in the persistent of left superior vena cava (**Figure 8**).

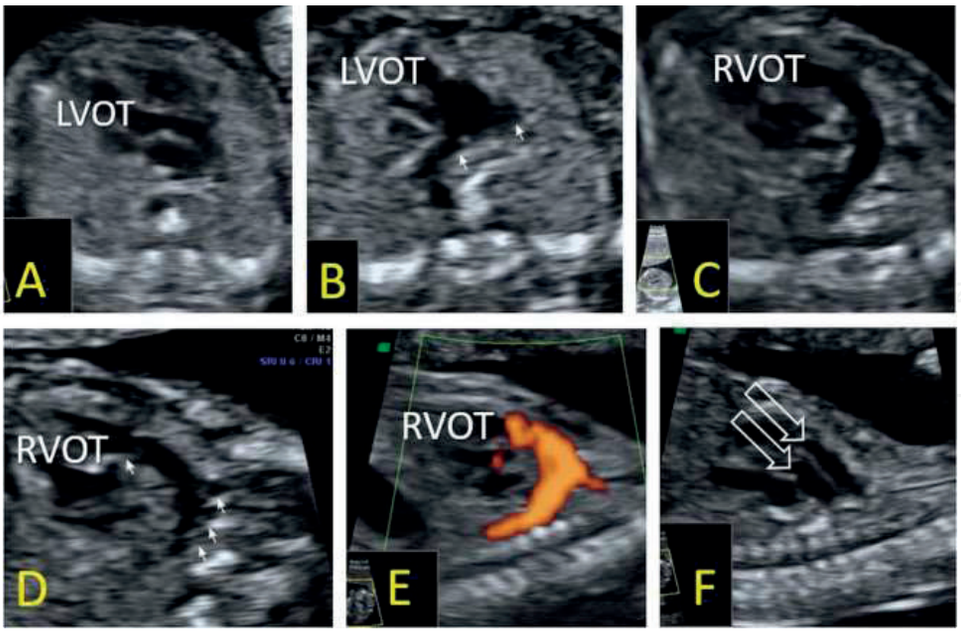

Figure 18. Transposition of the great arteries. (A): Emergence of the vessel arising from the left ventricle, showing early branching (B) that suggest pulmonary outflow tract. (C): Emergence of the vessel arising from the right ventricle with no evident branching in the transversal plane. (D): Sagittal view of the thorax showing branching characteristic to aortic arch of the vessel arising from the anterior ventricle in gray scale and after power Doppler is applied (E). (F): Parallel course of the great vessels.

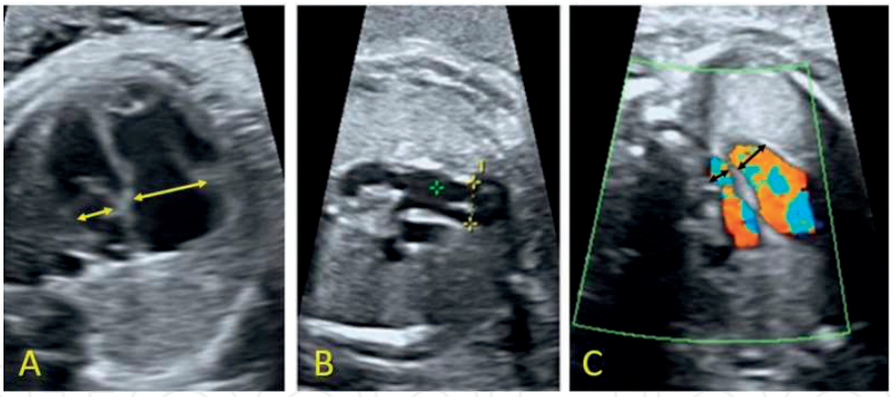

Figure 19. Discrepancy between the large right ventricle, pulmonary root and arterial duct and the diminutive left ventricle, aortic arch and isthmus in aortic coarctation. Calculations for mitral and tricuspid valves (A), arterial arches (B), isthmus and ductus (C).

Absence of a normal "V"-sign confluence of the arterial arches can be used to detect aortic arch abnormalities: right aortic arch, double aortic arch (**Figure 22**) and interrupted aortic arch (**Figure 20**).

6. Aortic and ductal arches views

- *The aortic* and *ductal arches* are visualized in longitudinal planes aligned with the respective ventricular outflow tracts. Aorta origins from the middle of the heart, with a typical "hook" shape, with the neck vessels arising longitudinally (**Figure 23A**).

http://dx.doi.org/10.5772/intechopen.74077

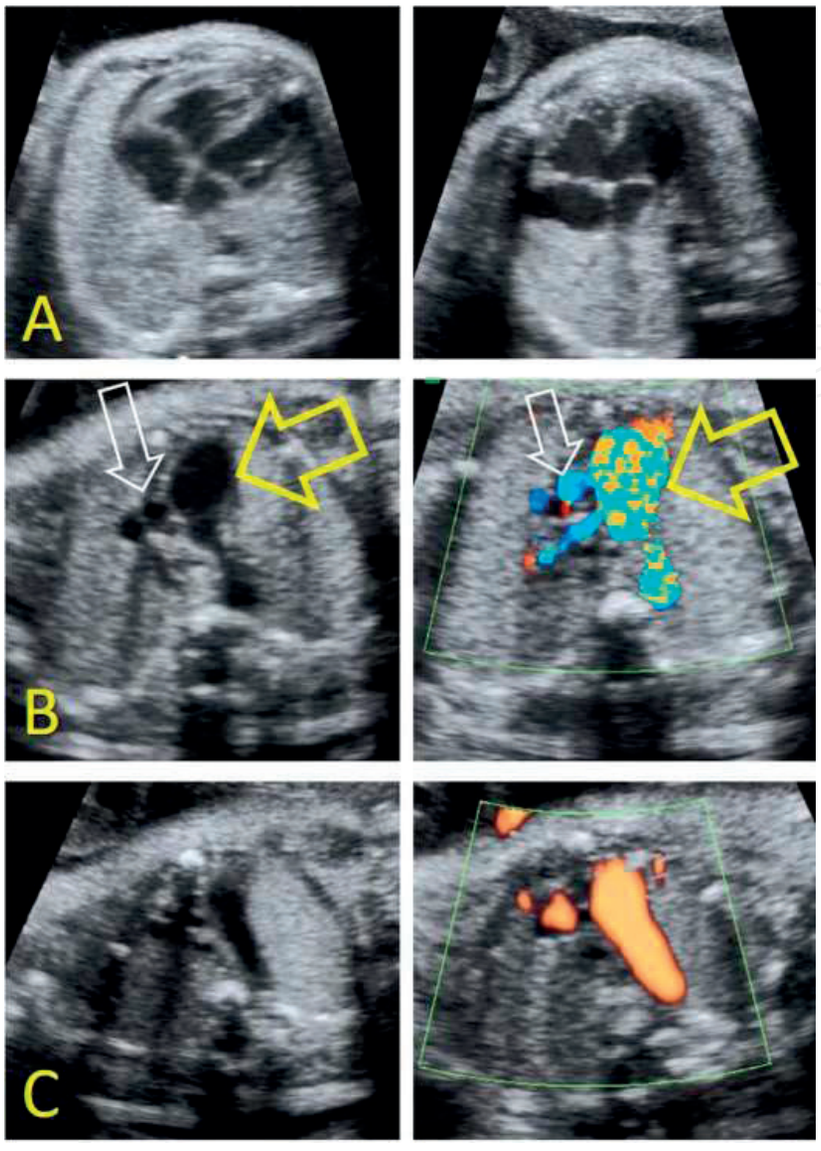

Figure 20. Interrupted aortic arch. (A): The ventricular discordance is not present, because of the septal defect, not evident in four-chamber views, but sub-aortic, when the entire septum is swept. (B): Enlarged pulmonary trunk (yellow arrow), and thin aorta (white arrow) in 3VT view. (C): Discontinuity of aortic arch in upper mediastinum axial planes.

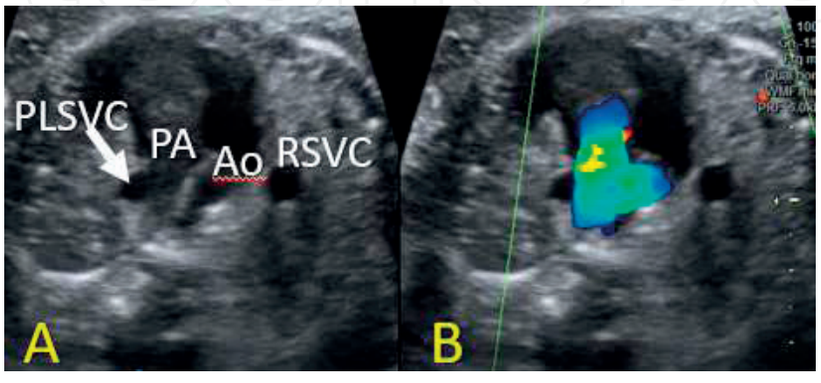

Figure 21. Persistent left superior vena cava (PLSCV), indicated with arrow in duplex gray-scale (A) and color Doppler (B) evaluation.

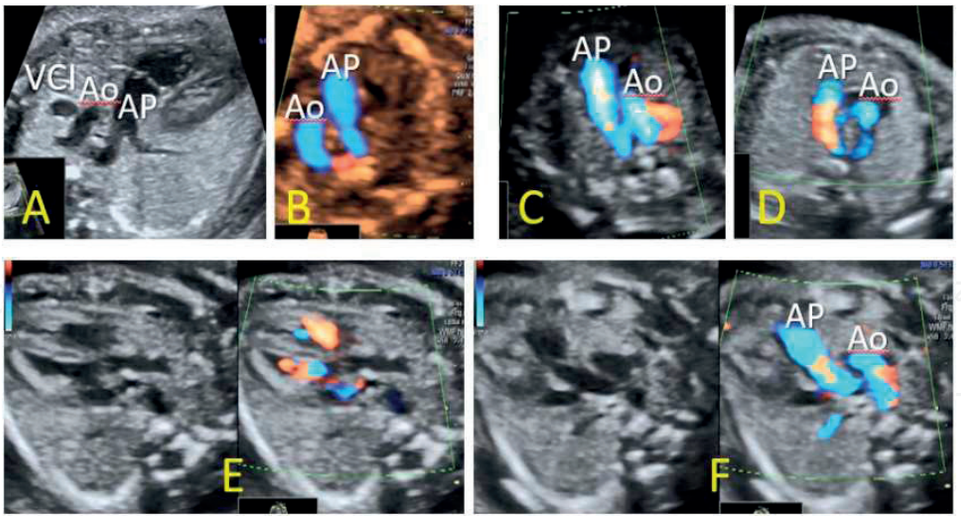

Figure 22. Right aortic arch (RAA) types. RAA and left ductus, forming a "U" shape of the arterial arches confluence as an almost complete vascular ring (A and B). Note the aorta coursing to the right of the spine, on the same side with superior vena cava (A), and a visible vascular incomplete ring behind the trachea. Double aortic arch, color Doppler evaluation (C and D) with complete vascular ring between the aortic branches. RAA with right ductus (E and F), described before with normal heart [44], duplex mode evaluation. Both arterial arches are directed to the right of the spine, resulting a "V"-shaped confluence on the right of the spine.

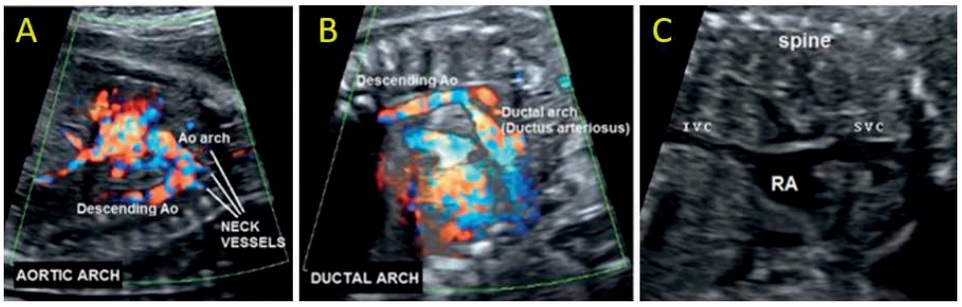

Figure 23. Aortic (A) and ductal (B) arches in longitudinal view. Note the differences mentioned in the text, regarding the origin, curvature and branching. (C): Bicaval view. IVC, inferior vena cava; SVC, superior vena cava; RA, right atrium.

A diminutive caliber accompanied by an altered shape may be present in aortic arch coarctation (**Figure 24A**) or stenosis (**Figure 16D**). Also, the course of the arch may be misshaped and interrupted, with lack of communication with the descending aorta, as in interrupted aortic arch (**Figure 24C**).

The vessel may appear irregular and thin, as in pulmonary stenosis (**Figure 24B**), or heavily dilated, as in aortic arch stenosis or interruption (**Figure 24D**). The ductus may be absent, as is usually in the most frequent variant of absent pulmonary valve syndrome-associated with tetralogy of Fallot. Another type of the syndrome—accompanied by tricuspid atresia, is characterized by a normal or narrowed ductus arteriosus, along the dysplastic right ventricle. Contrarily, the isolated type of absent pulmonary valve syndrome, with intact ventricular septum, associates a severe right ventricular hypertrophy with pulmonary artery and ductus arteriosus dilatation.

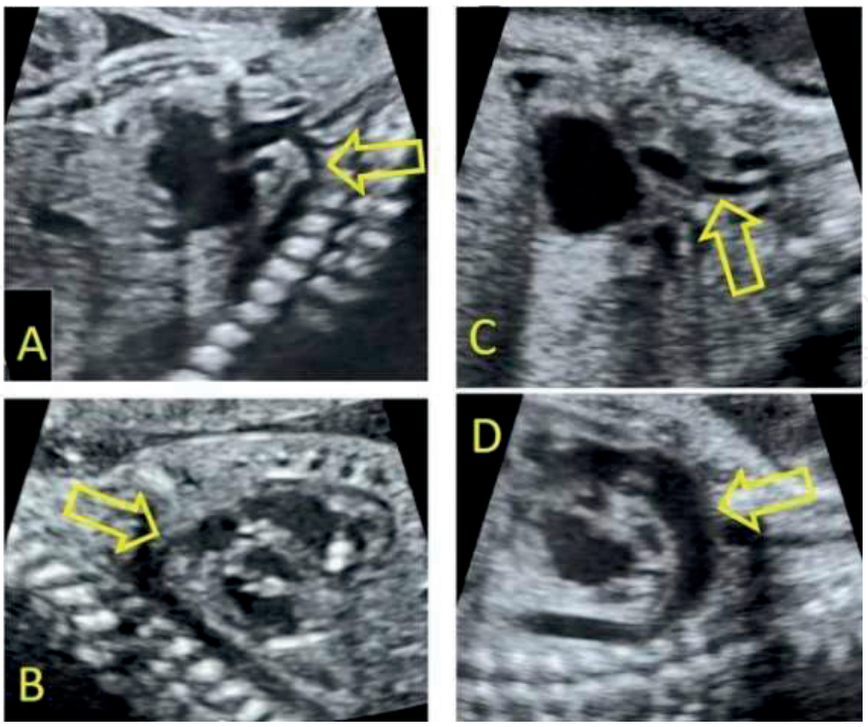

Figure 24. Pathologic aortic and ductal arches in longitudinal view. (A): Aortic coarctation with stenotic isthmus (arrow); (B): pulmonary valvular stenosis, with irregular course and stenotic ductal areas; (C and D): interrupted aortic arch, with ascending aorta that fails to curve, but courses straight cranially (C), and heavily enlarged ductal arch (D).

- *Superior and inferior vena cava views*/caval long-axis view/bicaval view is found longitudinally on the right of the spine, in line with the superior and inferior vena cava confluence with the right atrium (**Figure 23C**). The normal aspect is altered in fetal isomerism, interrupted inferior vena cava or persistent left superior vena cava.

4. Doppler imaging

Color Doppler and *high definition directional power flow* sonography allows for a better understanding of the cardio-vascular anatomy and function [18, 45, 46], particularly in detecting regurgitation, small septal defects and first trimester anatomic and physiological features of heart, as presented below. The ductus venosus appearance, flow and connections depend on the Doppler identification and interrogation of this small vascular structure. Agenesis of ductus venosus was associated with a high incidence of cardio-vascular and genetic abnormalities (**Figures 25** and **26**).

Pulsed Doppler sonography is an adjunct to evaluate the cardiac rhythm, but also the blood flows at the level of various arteria or venous vascular sites and valves.

B-flow and classic power Doppler display in some cases greater sensitivity in imaging cardio-vascular blood flow, but they are not routinely used.

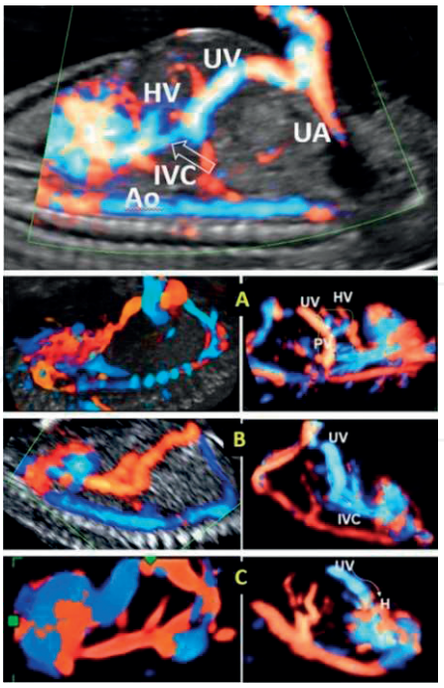

Figure 25. The upper image presents the normal appearance of ductus venosus in 2D color Doppler imaging. (A–C): Agenesis of ductus venosus: with hepatic (A), caval (B) and cardiac (C) drainage. UV, umbilical vein; IVC, inferior vena cava; H, heart; HV, hepatic veins; UA, umbilical artery; PV, portal vein; Ao, aorta.

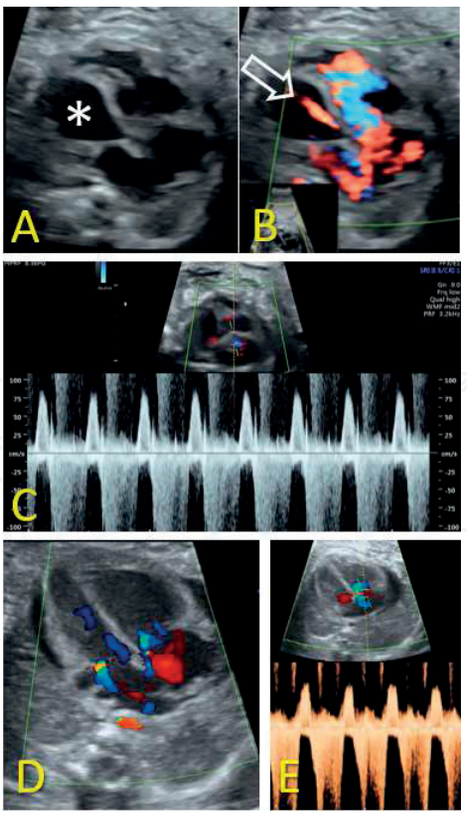

Figure 26. Applications of color and spectral Doppler. (A): Critical aortic stenosis with dysplastic left ventricle (*), atretic valve and aortic regurgitation (arrow, (B)). (C): Same case, tricuspid regurgitation, pulsed Doppler evaluation. (D): Atrioventricular valves regurgitation associated with cardiomegaly. (E): Same case, spectral Doppler evaluation of atrioventricular flow.

5. 4D spatiotemporal image correlation (STIC)

Volume datasets obtained with 4D STIC ultrasonography allow the evaluation of virtual planes not available for direct visualization with 2D technique, and facilitates the reconstruction of the spatial relationships between the cardio-vascular structures (**Figure 27**). This technology has the potential to increase the CHD detection rate by decreasing the dependency on sonographer skills and experience. However, due to the expensive costs and lack of specialists for training and interpretations, the technique is not routinely used.

In selected cases, it may offer important information as the comprehensive assessment of complex CHD cases [47–50] and the evaluation of cardiac function and quantification of fetal hemodynamic parameters, such as cardiac output [51].

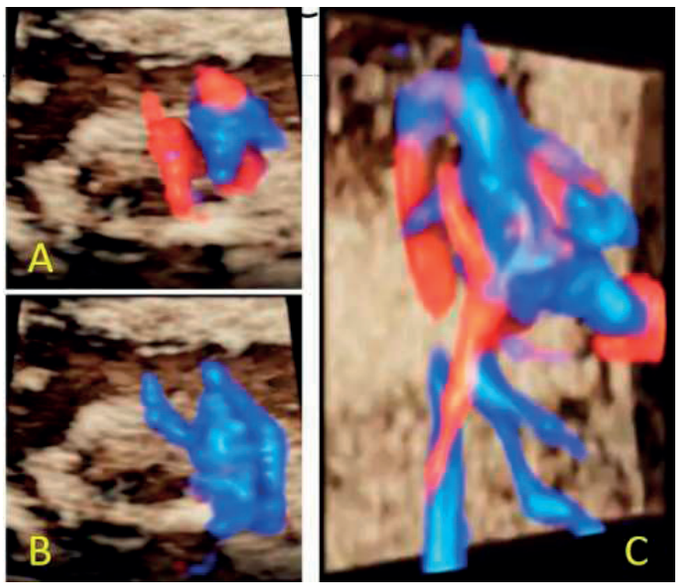

Figure 27. Double outlet right ventricle in 4D STIC. Axial planes show the origin of the great vessels (A) and the communication of the pulmonary artery with the left ventricle, due to a septal defect (B). Oblique longitudinal plane with the anterior origin of the two outflow tracts (C).

6. Cardiac function

It should be considered for suspected structural or functional cardiac anomalies [18, 19]. Some *qualitative* markers are identified during standard scanning: cardiomegaly, atrioventricular valve regurgitation, and hydrops. The *quantitative* assessment of heart function includes the study of myocardial movement such as tissue Doppler, myocardial/ventricular strain, strain rate imaging, fractional shortening and the myocardial performance index [52–54].

7. Efficiency of the fetal cardiac scan

Although the most frequent congenital malformations, CHDs are among the most frequently missed [18, 55]. The efficiency of the cardiac scan is reported with great variation, depending

on the scanning protocol, examiner experience, equipment quality and scanning conditions [18, 56–58]. It appears that the use of 4CV alone detects up to 77% of CHD, while adding OTV increases prenatal detection to 83–92% of major abnormalities.

8. Early evaluation of the fetal heart, at the first trimester (FT) morphogenetic scan

Congenital heart defects appear during the first 8 weeks of the fetus development, thus cardiac sonography at the genetic scan, during 11–13 gestational weeks (GW) is feasible (**Figure 28**) and identifies numerous abnormalities (**Figures 29–35**) [59–61]. The rate of complete cardiac evaluation increases with gestational age, from 20% at 11GW, to more than 92% at 13–15 GW, especially when transvaginal route was used [62, 63].

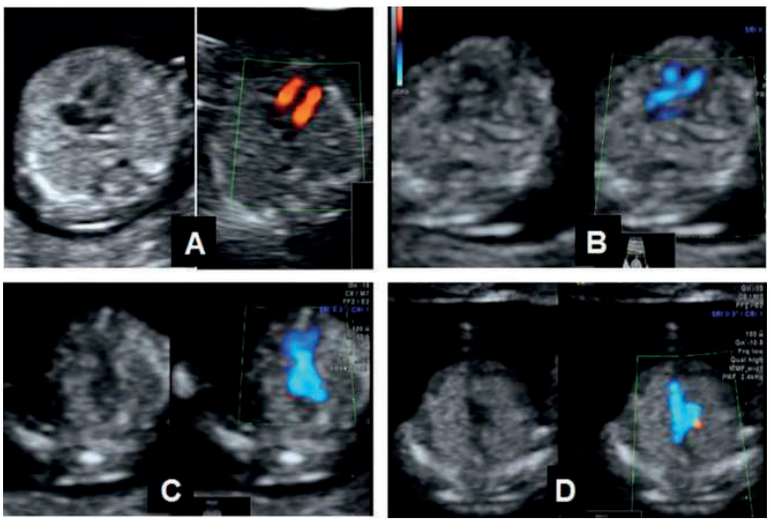

Figure 28. FT cardiac sweep of a normal heart, duplex mode. (A): 4CV plane: gray-scale imaging shows, crux cordis and pulmonary veins entering left atrium; color Doppler imaging shows equal atrioventricular flow and no flow between ventricles. (B): LVOT plane with the aortic emergence, septoaortic continuity and aortic flow. (C): Crossing of the great vessels. (D): 3VT plane – the confluence of arterial arches on left of spine with normal direction and equal flow.

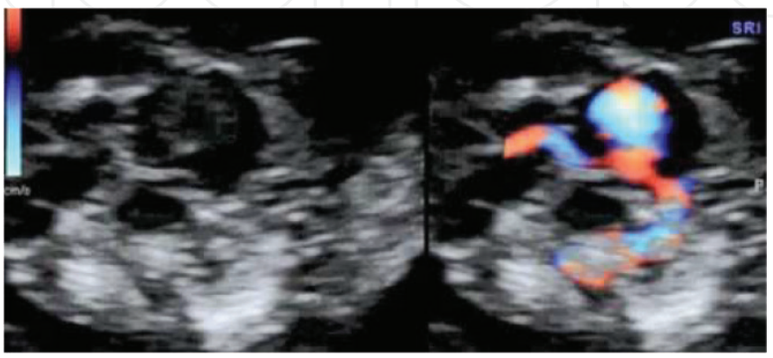

Figure 29. Monoventricular heart.

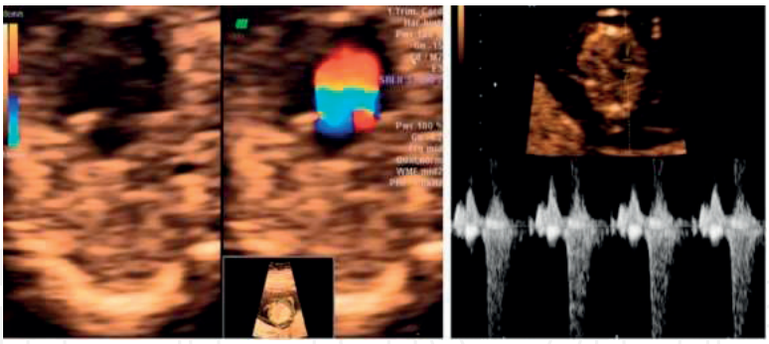

Figure 30. Atrioventricular septal defect. Thickened common valve, large communication between the cardiac chambers, absence of crux cordis and regurgitation.

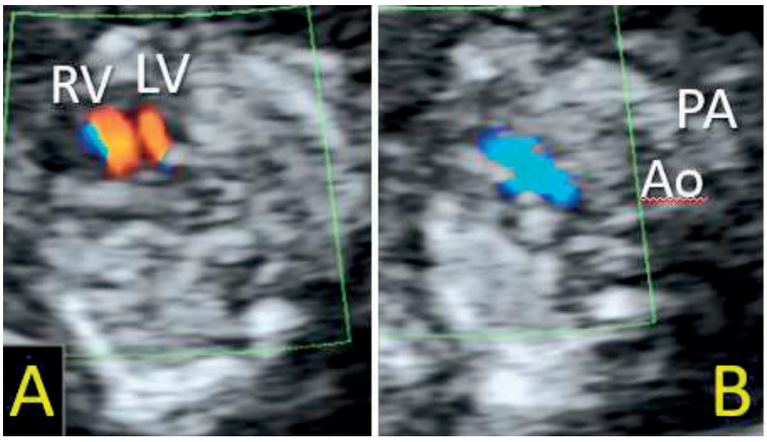

Figure 31. Hypoplastic left heart. A diminutive left ventricle (A) and aorta (B) are identified with the aid of color Doppler. RV, left ventricle; LV, left ventricle; PA, pulmonary artery; Ao, aorta.

Regarding the *imaging technique*, gray scale is the basis of a reliable fetal cardiac scan in the ST, but much less informative in the FT [64].

For safety reasons, routine use of pulsed color Doppler is advised against in the FT [65], although tricuspid and ductus venosus flows are commonly used [66–72] and color Doppler improves early visualization of cardio-vascular features, due to the low discrimination of the heart structures in gray-scale mode [73–75], while respecting the ALARA principle (As Low As Reasonably Achievable) [76].

At a lesser extent, the FT *examination protocol* is similar to the second trimester cardiac scan [77, 78], as presented in **Figure 28**. 4D-STIC is feasible in the FT and likely to improve CHD detection in expert hands.

The *efficiency* of FT cardiac scan varies widely (detection rate 5.6–90%), depending on the protocol used, population risk and scanning route (TV, TA or both). High detection rates for major CHD were reported even in unselected or low risk population 80–90%, when using an extended standardized protocol [74, 75]. A systematic review of the literature [79] reported a pooled sensitivity and specificity of 85% (95% CI, 78–90%) and 99% (95% CI, 98–100%),

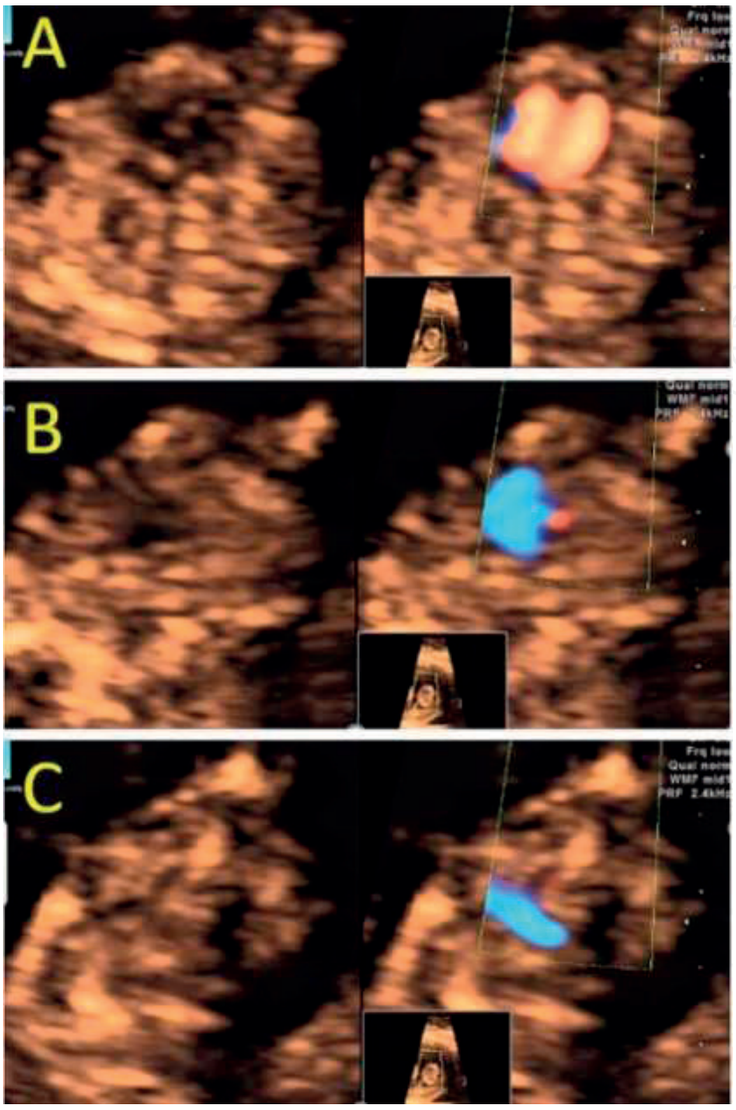

Figure 32. Transposition of great arteries. Inapparent four-chamber view (A), with parallel course of the arterial arches (B) and the impression of only one arterial arch at the level of 3VT view (C).

respectively. Thus, FT cardiac scan has a high accuracy in major CHD detection and a reasonable accuracy to diagnose normal heart. We should underline during parents counseling that normal fetal cardiac features examinations at any time of pregnancy do not exclude CHD, as some diseases evolve in utero and become apparent later during pregnancy: coarctation of aorta, pulmonary stenosis, tetralogy of Fallot, hypoplastic left heart syndrome, cardiomyopathy or cardiac tumors [80–83]. Ventricular septal defects are the earliest missed lesions because of the small size of the lesion and low flow velocities in the FT. A normal cardiac scan in the FT should not be considered a replacement for the second trimester echocardiography.

Markers for cardiac abnormalities (**Figure 36**) may also be useful in early pregnancy, as increased nuchal translucency (NT) and abnormal ductus venosus and tricuspid flows. Increased *NT* was associated with cardiac dysfunction and abnormalities, even in chromosomally normal fetuses, but not obviously related to any particular type of cardiac anomaly [84–86]. The prevalence of CHD when NT is the 95th percentile is up to 20% [87] and about six times higher

http://dx.doi.org/10.5772/intechopen.74077

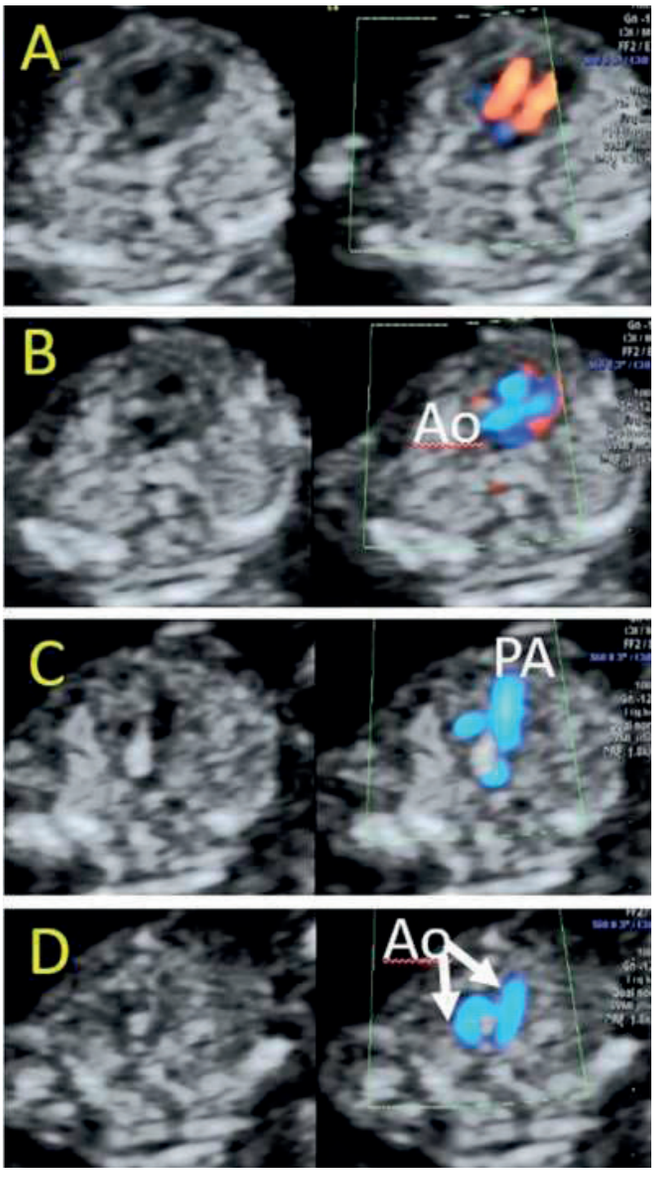

Figure 33. Double aortic arch. Four-chamber view with normal appearance (A), normal emergence of the aorta (B) and pulmonary artery (C), with the aorta coursing to the right of the spine and dividing in two branches that form a vascular ring around the trachea (D).

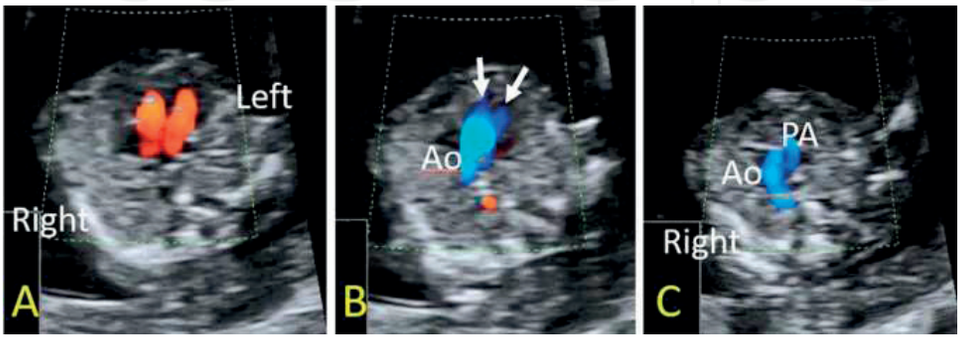

Figure 34. Tetralogy of Fallot with right aortic arch. (A): Normal appearance of atrioventricular flows; (B): overriding aorta; (C): aorta coursing to the right of the spine along the diminutive pulmonary artery.

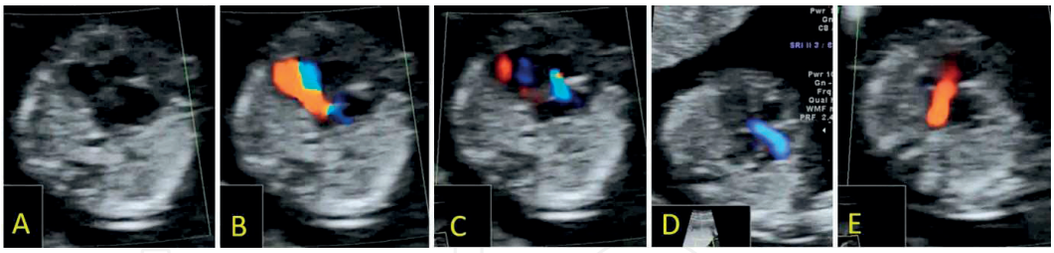

Figure 35. Hypoplastic right heart syndrome. Tricuspid atresia with intact septum. (A): Dysplastic thickened tricuspid valve in 4CV assessment, with lack of antegrade blood flow (B) and regurgitation (C). Normal aortic flow is visualized (D), and reversed ductal flow (E), by using color Doppler.

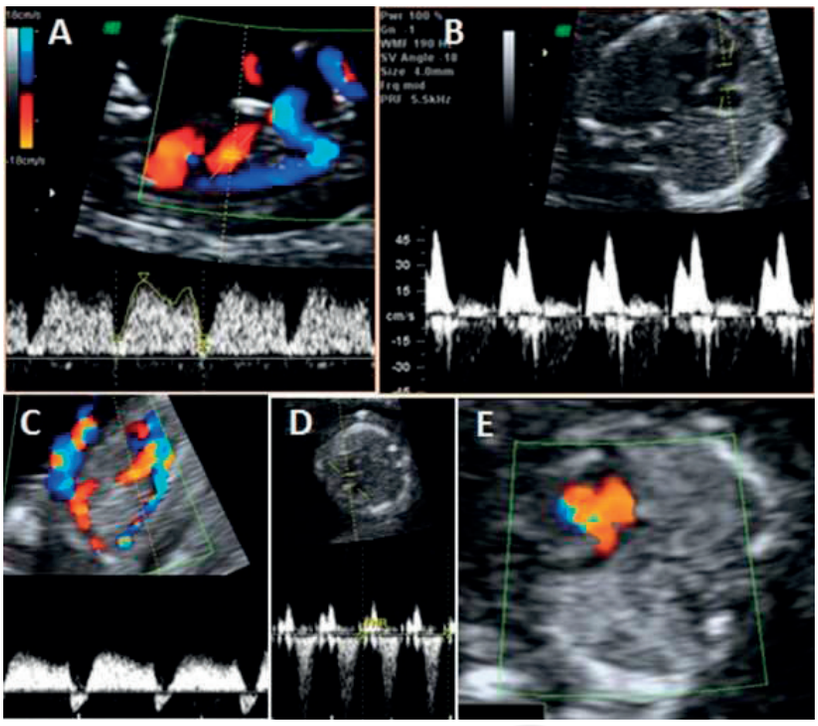

Figure 36. Normal flows at the pulsed Doppler interrogation of ductus venosus (A) and tricuspid valve (B). Ductus venosus with reversed a-wave (C) and tricuspid regurgitation (D) in fetus with atrioventricular septal defect (E).

than unselected population for NT ≥99th percentile [88]. Still, NT measurement is not a reliable screening test for CHD during FT, because of the overall low detection rates for CHD (around 15%) in unselected or low-risk populations [89, 90].

The performance of early screening for CHD achieved by measurement of fetal NT is improved by the assessment of ductus venosus and tricuspid valve flow pattern. In fetuses with enlarged NT (above 95 centile) and *absent or reversed a-wave in DV flow* the risk for major CHD is tripled [91]. The finding of reversed a-wave in chromosomally normal fetuses increases by almost 10 times the risk of CHD, with a predominance of right-heart anomalies regardless of the measurement of NT [86]. Also, chromosomally normal fetuses with *tricuspid valve regurgitation* have an 8-fold increased risk for CHD [92, 93].

Author details

Dominic Gabriel Iliescu[1], Ștefania Tudorache[1], Dragos Nemescu[2]*, Monica Mihaela Cirstoiu[3], Simona Vlădăreanu[4], Claudiu Marginean[5], Iuliana Ceausu[3], Daniel Muresan[6], Marius Calomfirescu Vicea[7], Mona Elena Zvanca[3], Cezara Muresan[8], Laura Monica Cara[9], Ciprian Laurentiu Patru[1], Roxana Cristina Drăgușin[1] and Maria Sorop-Florea[1]

*Address all correspondence to: dnemescu@yahoo.com

1 Department of Obstetrics and Gynaecology, University of Medicine and Pharmacy, Craiova, Romania

2 Department of Obstetrics and Gynaecology, University of Medicine and Pharmacy, "Gr.T.Popa", Iasi, Romania

3 Department of Obstetrics-Gynecology, University of Medicine and Pharmacy, Bucharest, Romania

4 Department of Neonatology, University of Medicine and Pharmacy, "Carol Davila", Bucharest, Romania

5 Department of Obstetrics and Gynaecology, University of Medicine and Pharmacy, Targu-Mures, Romania

6 Department of Obstetrics and Gynaecology, University of Medicine and Pharmacy, "Iuliu Hatieganu", Cluj-Napoca, Romania

7 Secretary, Romanian Society of Ultrasound in Obstetrics and Gynecology, Bucharest, Romania

8 Department of Obstetrics and Gynaecology, University of Medicine and Pharmacy, "Victor Babes", Timisoara, Romania

9 Department of Public Health, University of Medicine and Pharmacy, Craiova, Romania

References

[1] Rosano A, Botto LD, Botting B. Infant mortality and congenital anomalies from 1950 to 1994: An international perspective. Journal of Epidemiology and Community Health. 2000;**54**:660-666

[2] Donofrio MT, Moon-Grady AJ, Hornberger LK, et al. Diagnosis and treatment of fetal cardiac disease a scientific statement from the American Heart Association. Circulation. 2014;**129**:2183-2242

[3] Chenni N, Lacroze V, Pouet C, Fraisse A, Kreitmann B, Gamerre M, Boubli L, D'Ercole C. Fetal heart disease and interruption of pregnancy: Factors influencing the parental decision-making process. Prenatal Diagnosis. 2012 Feb;**32**(2):168-172. DOI: 10.1002/pd.2923

[4] Rasiah SV, Ewer AK, Miller P, Kilby MD. Prenatal diagnosis, management and outcome of fetal dysrhythmia: A tertiary fetal medicine centre experience over an eight-year period. Fetal Diagnosis and Therapy. 2011;**30**(2):122-127

[5] McLaughlin ES, Schlosser BA, Border WL. Fetal diagnostics and Fetal intervention. Clinics in Perinatology. 2016 Mar;**43**(1):23-38

[6] Yuan SM. Fetal cardiac interventions. Pediatrics and Neonatology. 2015 Apr;**56**(2):81-87

[7] Schidlow DN, Tworetzky W, Wilkins-Haug LE. Percutaneous fetal cardiac interventions for structural heart disease. American Journal of Perinatology. 2014 Aug;**31**(7):629-636

[8] Chiappa E. The impact of prenatal diagnosis of congenital heart disease on pediatric cardiology and cardiac surgery. Journal of Cardiovascular Medicine (Hagerstown, Md.). 2007 Jan;**8**(1):12-16

[9] Franklin O, Burch M, Manning N, Sleeman K, Gould S, Archer N. Prenatal diagnosis of coarctation of the aorta improves survival and reduces morbidity. Heart. 2002;**87**:67-69

[10] Mahle WT, Clancy RR, McGaurn SP, Goin JE, Clark BJ. Impact of prenatal diagnosis on survival and early neurologic morbidity in neonates with the hypoplastic left heart syndrome. Pediatrics. 2001;**107**:1277-1282

[11] Bonnet D, Coltri A, Butera G, Fermont L, Le Bidois J, Kachaner J, Sidi D. Detection of transposition of the great arteries in fetuses reduces neonatal morbidity and mortality. Circulation. 1999;**99**:916-918

[12] Jenkins KJ, Correa A, Feinstein JA, et al. Non-inherited risk factors and congenital cardiovascular defects: Current knowledge: A scientific statement from the American Heart Association Council on cardiovascular disease in the young: Endorsed by the American Academy of Pediatrics. Circulation. 2007;**15**:2995-3014

[13] Ferencz C, Correa-Villasenor A, Loffredo CA, editors. Genetic and Environmental Risk Factors of Major Cardiovascular Malformations: The Baltimore-Washington Infant Study: 1981-1989. Armonk, NY: Futura Publishing Co; 1997

[14] Williams LJ, Correa A, Rasmussen S. Maternal lifestyle factors and risk for ventricular septal defects. Birth Defects Research. Part A, Clinical and Molecular Teratology. 2004;**70**:59-64

[15] Shaw GM, Nelson V, Iovannisci DM, Finnell RH, Lammer EJ. Maternal occupational chemical exposures and biotransformation genotypes as risk factors for selected congenital anomalies. American Journal of Epidemiology. 2003;**157**:75-484

[16] Carmichael SL, Shaw GM. Maternal life event stress and congenital anomalies. Epidemiology. 2000;**11**:0-35

[17] Botto LD, Mulinare J, Erickson JD. Occurrence of congenital heart defects in relation to maternal multivitamin use. American Journal of Epidemiology. 2000;**151**:878-884

[18] International Society of Ultrasound in Obstetrics and Gynecology, Carvalho JS, Allan LD, Chaoui R, Copel JA, DeVore GR, Hecher K, Lee W, Munoz H, Paladini D, Tutschek B, Yagel S. ISUOG Practice Guidelines (updated): sonographic screening examination of the fetal heart. Ultrasound in Obstetrics & Gynecology. 2013 Mar;**41**(3):348-359

[19] American Institute of Ultrasound in Medicine. AIUM practice guideline for the performance of fetal echocardiography. Journal of Ultrasound in Medicine. 2013 Jun; **32**(6):1067-1082

[20] Small M, Copel JA. Indications for fetal echocardiography. Pediatric Cardiology. 2004; **25**:210-222

[21] Smrcek JM, Berg C, Geipel A, Fimmers R, Axt-Fliedner R, Diedrich K, Gembruch U. Detection rate of early Fetal echocardiography and in utero development of congenital heart defects. Journal of Ultrasound in Medicine. 2005;**25**:187-196

[22] Volpe P, De Robertis V, Campobasso G, Tempesta A. Diagnosis of congenital heart disease by early and second-trimester Fetal echocardiography. Journal of Ultrasound in Medicine. 2012;**31**:563-568

[23] Carvalho JS, Ho SY, Shinebourne EA. Sequential segmental analysis in complex fetal cardiac abnormalities: A logical approach to diagnosis. Ultrasound in Obstetrics & Gynecology. 2005;**26**:105-111

[24] Wood D, Respondek-Liberska M, Puerto B, Weiner S. Perinatal echocardiography: Protocols for evaluating the fetal and neonatal heart. World Association of Perinatal Medicine Ultrasonography Working Group. Journal of Perinatal Medicine. 2009;**37**(1):5-11

[25] Yagel S, Cohen SM, Achiron R. Examination of the fetal heart by five short-axis views: A proposed screening method for comprehensive cardiac evaluation. Ultrasound in Obstetrics & Gynecology. 2001 May;**17**(5):367-369

[26] Available from: http://www.smgebooks.com/echocardiography/chapters/ECHO-16-05.pdf. p. 7

[27] Crane JM, Ash K, Fink N, Desjardins C. Abnormal fetal cardiac axis in the detection of intrathoracic anomalies and congenital heart disease. Ultrasound in Obstetrics & Gynecology. 1997 Aug;**10**(2):90-93

[28] Abuhamad A, Chaoui R. A Practical Guide to Fetal Echocardiography, Normal and Abnormal Hearts. Philadelphia, United States: Lippincott Williams and Wilkins; 2009. ISBN: 0781797578

[29] Schneider C, McCrindle BW, Carvalho JS, Hornberger LK, McCarthy KP, Daubeney PE. Development of z-scores for fetal cardiac dimensions from echocardiography. Ultrasound in Obstetrics & Gynecology. 2005;**26**:599-605

[30] Lee W, Riggs T, Amula V, et al. Fetal echocardiography: z-Score reference ranges for a large patient population. Ultrasound in Obstetrics & Gynecology. 2010;**35**:28-34

[31] Chobot V, Hornberger LK, Hange-Ansert S, Sahn DJ. Prenatal detection of restrictive foramen ovale. Journal of the American Society of Echocardiography. 1990;**3**:15-19

[32] Sharland G, Lockhart S. Isolated pericardial effusion: An indication for fetal karyotyping? Ultrasound in Obstetrics & Gynecology. 1995 Jul;**6**(1):29-32

[33] Slesnick TC, Ayres NA, Altman CA, Bezold LI, Eidem BW, Fraley JK, Kung GC, McMahon CJ, Pignatelli RH, Kovalchin JP. Characteristics and outcomes of fetuses with pericardial effusions. The American Journal of Cardiology. 2005 Aug 15;**96**(4):599-601

[34] Tudorache S, Chiuţu LC, Iliescu DG, Georgescu R, Stoica GA, Simionescu CE, Georgescu EF, Nemeş RN. Prenatal diagnosis and perinatal outcome in congenital diaphragmatic hernia. Single tertiary center report. Romanian Journal of Morphology and Embryology. 2014;**55**(3):823-833

[35] Chaoui R. The four-chamber view: Four reasons why it seems to fail in screening for cardiac abnormalities and suggestions to improve detection rate. Ultrasound in Obstetrics & Gynecology. 2003;**22**:3-10

[36] Ultrasound Screening: Supplement to Ultrasound Screening for Fetal Abnormalities. Available form: http://www.rcog.org.uk/print/womenshealth/clinical-guidance/ultrasound-screeningRCOG2011

[37] Israel Society of Ultrasound in Obstetrics and Gynecology. Available form: http://www.isuog.org.il/main/siteNew/?page=&action=sidLink&stld=301

[38] DeVore GR. The aortic and pulmonary outflow tract screening examination in the human fetus. Journal of Ultrasound in Medicine. 1992;**11**:345-348

[39] Del Bianco A, Russo S, Lacerenza N, et al. Four-chamber view plus three-vessel and trachea view for a complete evaluation of the fetal heart during the second trimester [published erratum appears in J Perinat Med 2006; 34:509]. Journal of Perinatal Medicine. 2006;**34**:309-312

[40] Achiron R, Glaser J, Gelernter I, Hegesh J, Yagel S. Extended fetal echocardiographic examination for detecting cardiac malformations in low risk pregnancies. British Medical Journal. 1992;**304**(3828):671-674

[41] Tonni G, Rosignoli L, Cariati E, Martins W, Miyague A, Bruns R, Araujo Jr E. Fetal thymus: Visualization rate and volume by integrating 2D- and 3D-ultrasound during 2nd trimester echocardiography. The Journal of Maternal-Fetal & Neonatal Medicine. 2015 Sep;**11**:1-6

[42] Pasquini L, Mellander M, Seale A, Matsui H, Roughton M, Ho SY, Gardiner HM. Z-scores of the fetal aortic isthmus and duct: An aid to assessing arch hypoplasia. Ultrasound in Obstetrics & Gynecology. 2007 Jun;**29**(6):628-633

[43] Jowett V, Aparicio P, Santhakumaran S, Seale A, Jicinska H, Gardiner HM. Sonographic predictors of surgery in fetal coarctation of the aorta. Ultrasound in Obstetrics & Gynecology. 2012 Jul;**40**(1):47-54

[44] Iliescu DG, Comanescu AC, Tudorache S, Cernea N. Right aortic arch with patent right ductus arteriosus and normal heart. Ultrasound in Obstetrics & Gynecology. 2012 Jul; **40**(1):115-116

[45] Alves Rocha L, Araujo Júnior E, Rolo LC, Barros FS, Silva KP, Martinez LH, Nardozza LM, Moron AF. Screening of congenital heart disease in the second trimester of pregnancy: Current knowledge and new perspectives to the clinical practice. Cardiology in the Young. 2014 Jun;**24**(3):388-396

[46] Gembruch U, Chatterjee MS, Bald R, Redel DA, Hansmann M. Color Doppler flow mapping of fetal heart. Journal of Perinatal Medicine. 1991;**19**(1-2):27-32

[47] Espinoza J, Gonçalves LF, Lee W, Mazor M, Romero R. A novel method to improve prenatal diagnosis of abnormal systemic venous connections using three- and four-dimensional ultrasonography and "inversion mode". Ultrasound in Obstetrics & Gynecology. 2005;**25**:428-434

[48] Volpe P, Campobasso G, De Robertis V, Di Paolo S, Caruso G, Stanziano A, Volpe N, Gentile M. Two- and four-dimensional echocardiography with B-flow imaging and spatiotemporal image correlation in prenatal diagnosis of isolated total anomalous pulmonary venous connection. Ultrasound in Obstetrics & Gynecology. 2007;**30**:830-837

[49] Paladini D, Volpe P, Sglavo G, Vassallo M, De Robertis V, Marasini M, Russo MG. Transposition of the great arteries in the fetus: Assessment of the spatial relationships of the arterial trunks by four-dimensional echocardiography. Ultrasound in Obstetrics & Gynecology. 2008;**31**:271-276

[50] Volpe P, Tuo G, De Robertis V, Campobasso G, Marasini M, Tempesta A, Gentile M, Rembouskos G. Fetal interrupted aortic arch: 2D–4D echocardiography, associations and outcome. Ultrasound in Obstetrics & Gynecology. 2010;**35**:302-309

[51] Molina FS, Faro C, Sotiriadis A, Daklis T, Nicolaides KH. Heart stroke volume and cardiac output by four-dimensional ultrasound in normal fetuses. Ultrasound in Obstetrics & Gynecology. 2008;**32**:181-187

[52] DeVore GR. Assessing fetal cardiac ventricular function. Seminars in Fetal & Neonatal Medicine. 2005;**10**:515-541

[53] Larsen LU, Petersen OB, Norrild K, Sorensen K, Uldbjerg N, Sloth E. Strain rate derived for color Doppler myocardial imaging for assessment of fetal cardiac function. Ultrasound in Obstetrics & Gynecology. 2006;**27**:210-213

[54] Hernandez-Andrade E, López-Tenorio J, Figueroa-Diesel H, et al. A modified myocardial performance (Tei) index based on the use of valve clicks improves reproducibility of fetal left cardiac functionassessment. Ultrasound in Obstetrics & Gynecology. 2005;**26**:227-232

[55] Crane JP, LeFevre ML, Winborn RC, Evans JK, Ewigman BG, Bain RP, Frigoletto FD, McNellis D. A randomized trial of prenatal ultrasonographic screening: Impact on the detection, management, and outcome of anomalous fetuses. The RADIUS Study Group. American Journal of Obstetrics and Gynecology. 1994;**171**:392-399

[56] Wood D, Respondek-Liberska M, Puerto B, Weiner S. Perinatal echocardiography: Protocols for evaluating the fetal and neonatal heart. World Association of Perinatal Medicine Ultrasonography Working Group. Journal of Perinatal Medicine. 2009; **37**(1):5-11

[57] Simpson LL. Screening for congenital heart disease. Obstetrics and Gynecology Clinics of North America. 2004;**31**:51-59

[58] Ahmed B, Stanojevic M, Kopjar T. Accuracy of the Fetal echocardiography in the high risk pregnancies. Donald School Journal of Ultrasound in Obstetrics and Gynecology. 2007 Jan–Mar;**1**(1):86-95

[59] Huggon IC, Ghi T, Cook AC, Zosmer N, Allan LD, Nicolaides KH. Fetal cardiac abnormalities identified prior to 14 weeks' gestation. Ultrasound in Obstetrics & Gynecology. 2002;**20**:22-29

[60] Carvalho JS, Moscoso G, Tekay A, Campbell S, Thilaganathan B, Shinebourne EA. Clinical impact of first and early second trimester fetal echocardiography on high risk pregnancies. Heart. 2004;**90**:921-926

[61] Taipale P, Ammala M, Salonen R, Hilesmaa V. Two-stage ultrasonography in screening for fetal anomalies at 13-14 and 18-22 weeks of gestation. Acta Obstetricia et Gynecologica Scandinavica. 2004;**83**:1141-1146

[62] Souka AP, Pilalis A, Kavalakis Y, Kosmas Y, Antsaklis P, Antsaklis A. Assessment of fetal anatomy at the 11-14-week ultrasound examination. Ultrasound in Obstetrics & Gynecology. 2004;**24**:730-734

[63] Smrcek JM, Berg C, Geipel A, Fimmers R, Axt-Fliedner R, Diedrich K, Gembruch U. Detection rate of early Fetal echocardiography and in utero development of congenital heart defects. Journal of Ultrasound in Medicine. 2005;**25**:187-196

[64] Tudorache S, Cara M, Iliescu DG, Novac L, Nicolae C. First trimester two- and four-dimensional cardiac scan: Intra- and interobserver agreement, comparison between methods and benefits of color Doppler technique. Ultrasound Obstetrics & Gynecology. 2013 Dec;**42**(6):659-68

[65] Tudorache S, Cara M, Iliescu DG, Novac L, Cernea N. First trimester two- and four-dimensional cardiac scan: Intra- and interobserver agreement, comparison between methods and benefits of color Doppler technique. Ultrasound in Obstetrics & Gynecology. 2013 Dec;**42**(6):659-668

[66] Chelemen T, Syngelaki A, Maiz N, Allan L, Nicolaides KH. Contribution of ductus venosus Doppler in first-trimester screening for major cardiac defects. Fetal Diagnosis and Therapy. 2011;**29**(2):127-134

[67] Borrell A, Perez M, Figueras F, Meler E, Gonce A, Gratacos E. Reliability analysis on ductus venosus assessment at 11-14 weeks' gestation in a high-risk population. Prenatal Diagnosis. May 2007;**27**(5):442-446

[68] Huggon IC, DeFigueiredo DB, Allan LD. Tricuspid regurgitation in the diagnosis of chromosomal anomalies in the fetus at 11-14 weeks of gestation. Heart. 2003;**89**:1071-1073

[69] Faiola S, Tsoi S, Huggon IC, Allan LD, Nicolaides KH. Likelihood ratio for trisomy 21 in fetuses with tricuspid regurgitation at the 11 to 13+6-week scan. Ultrasound in Obstetrics & Gynecology. 2005;**26**:22-27

[70] Maiz N, Nicolaides KH. Ductus Venosus in the first trimester: Contribution to screening of chromosomal, cardiac defects and monochorionic twin complications. Fetal Diagnosis and Therapy. 2010;**28**:65-71

[71] Oh C, Harman C, Baschat A. Abnormal first-trimester ductus venosus blood flow: A risk factor for adverse outcome in fetuses with normal nuchal translucency. Ultrasound in Obstetrics & Gynecology. 2007;**30**:192-196

[72] Papatheodorou S, Evangelou E, Makrydimas G, Ioannidis J. First-trimester ductus venosus screening for cardiac defects: A meta-analysis. BJOG : An International Journal of Obstetrics and Gynaecology. 2011;**118**:1438-1445

[73] Volpe P, De Robertis V, Campobasso G, Tempesta A. Diagnosis of congenital heart disease by early and second-trimester Fetal echocardiography. Journal of Ultrasound in Medicine. 2012;**31**:563-568

[74] Becker R, Albig M, Gasiorek-Wiens A, Entezami M, Knoll U, Wegner RD. The potential of first trimester anomaly scan and first trimester fetal echocardiography as screening procedures in a medium risk population. The Journal of Obstetrics and Gynecology of India. 2005 May/June;**55**(3):228-230

[75] Iliescu D, Tudorache S, Comanescu A, Antsaklis P, Cotarcea S, Novac L, Cernea N, Antsaklis A. Improved detection rate of structural abnormalities in the first trimester using an extended examination protocol. Ultrasound in Obstetrics & Gynecology. 2013 Sep;**42**(3):300-309

[76] Nemescu D, Berescu A. Acoustic output measured by thermal and mechanical indices during fetal echocardiography at the time of the first trimester scan. Ultrasound in Medicine & Biology. 2015 Jan;**41**(1):35-39

[77] Iliescu D, Cara M, Tudorache S, Antsaklis P, Ceausu I, Paulescu D, Novac L, Cernea N, Antsaklis A. Challenges in sonographic detection of fetal major structural abnormalities at the first trimester anomaly scan. Donald School Journal of Ultrasound in Obstetrics & Gynecology. 2015;**9**(3):239-259

[78] Roxana D, Florea M, Iliescu D, Cotarcea S, Tudorache S, Liliana N, Cernea N. The contribution and the importance of modern ultrasound techniques in the diagnosis of major structural abnormalities in the first trimester. Current Health Sciences Journal. 2012;**38**:1

[79] Rasiah SV, Publicover M, Ewer AK, Khan KS, Kilby MD, Zamora J. A systematic review of the accuracy of first-trimester ultrasound examination for detecting major congenital heart disease. Ultrasound in Obstetrics & Gynecology. 2006;**28**:110-111

[80] Smrcek JM, Berg C, Geipel A, Fimmers R, Axt-Fliedner R, Diedrich K, Gembruch U. Detection rate of early Fetal echocardiography and in utero development of congenital heart defects. Journal of Ultrasound in Medicine. 2005;**25**:187-196

[81] Syngelaki A, Chelemen T, Dagklis T, Allan L, Nicolaides KH. Challenges in the diagnosis of fetal non-chromosomal abnormalities at 11-13 weeks. Prenatal Diagnosis. 2011; **31**(1):90-102

[82] Khalil A, Nicolaides KH. Fetal heart defects: Potential and pitfalls of first-trimester detection. Seminars in Fetal & Neonatal Medicine. 2013 Oct;**18**(5):251-260

[83] Simpson JM, Jones A, Callaghan N, Sharland GK. Accuracy and limitation of transabdominal fetal echocardiography at 12-15 weeks of gestation in a population at high risk of congenital heart disease. BJOG: An International Journal of Obstetrics and Gynaecology. 2000;**107**:1492-1497

[84] Souka AP, von Kaisenberg CS, Hyett JA, Sonek JD, Nicolaides KH. Increased nuchal translucency with normal karyotype. American Journal of Obstetrics and Gynecology. 2005:1005-1021

[85] Makrydimas G, Sotiriadis A, Huggon IC, Simpson J, Sharland, Carvalho JS, Daubeney PE, Ioannidis JPA. Nuchal translucency and fetal cardiac defects: A pooled analysis of major fetal echocardiography centers. American Journal of Obstetrics and Gynecology. 2005;192:89-95

[86] Clur SA, Ottenkamp J, Bilardo CM. The nuchal translucency and the fetal heart: A literature review. Prenatal Diagnosis. 2009;**29**:739-748

[87] Souka AP, von Kaisenberg CS, Hyett JA, Sonek JD, Nicolaides KH. Increased nuchal translucency with normal karyotype. American Journal of Obstetrics and Gynecology. 2005:1005-1021

[88] Bilardo CM, Timmerman E, Pajkrt E, van Maarle M. Increased nuchal translucency in euploid fetuses – what should we be telling the parents? Prenatal Diagnosis. 2010;**30**:93-102

[89] Mavrides E, Cobian-Sanchez F, Tekay A, Moscoso G, Campbell S, Thilaganathan B, Carvalho JS. Limitations of using first-trimester nuchal translucency measurement in routine screening for major congenital heart defects. Ultrasound in Obstetrics & Gynecology. 2001;**17**:106-110

[90] Simpson LL, Malone FD, Bianchi DW, Ball RH, Nyberg DA, Comstock CH, et al. Nuchal translucency and the risk of congenital heart disease. Obstetrics and Gynecology. 2007 Feb;**109**(2 Pt 1):376-383

[91] Maiz N, Nicolaides KH. Ductus Venosus in the first trimester: Contribution to screening of chromosomal, cardiac defects and monochorionic twin complications. Fetal Diagnosis and Therapy. 2010;**28**:65-71

[92] Faiola S, Tsoi S, Huggon IC, Allan LD, Nicolaides KH. Likelihood ratio for trisomy 21 in fetuses with tricuspid regurgitation at the 11 to 13+6-week scan. Ultrasound in Obstetrics & Gynecology. 2005;**26**:22-27

[93] Grande M, Arigita M, Borobio V, Jimenez JM, Fernandez S, Borrell A. First-trimester detection of structural abnormalities and the role of aneuploidy markers. Ultrasound in Obstetrics & Gynecology. 2012 Feb;**39**(2):157-163